Theses and Dissertations

May 2015

Descriptive Analyses of Pollen Surface Morphologies in the Model Systems Brassica Rapa and Arabidopsis Thaliana and Three Arabidopsis Pollen Wall Mutants By Scanning Electron Microscopy

Andrew B. Kirkpatrick
University of Wisconsin-Milwaukee

DESCRIPTIVE ANALYSES OF POLLEN SURFACE MORPHOLOGIES IN THE

MODEL SYSTEMS *BRASSICA RAPA* AND *ARABIDOPSIS THALIANA* AND THREE

ARABIDOPSIS POLLEN WALL MUTANTS BY SCANNING ELECTRON

MICROSCOPY

by

Andrew B. Kirkpatrick

A Thesis Submitted in

Partial Fulfillment of the

Requirements for the Degree of

Master of Science

in Biological Sciences

at

The University of Wisconsin – Milwaukee

May 2015

ABSTRACT

DESCRIPTIVE ANALYSES OF POLLEN SURFACE MORPHOLOGIES IN THE
MODEL SYSTEMS *BRASSICA RAPA* AND *ARABIDOPSIS THALIANA* AND THREE
ARABIDOPSIS POLLEN WALL MUTANTS BY SCANNING ELECTRON
MICROSCOPY

by

Andrew B. Kirkpatrick

The University of Wisconsin-Milwaukee, 2015
Under the Supervision of Dr. Heather A. Owen

The mechanisms behind the construction of the pollen wall are equally elaborate and

mysterious. Previous studies primarily used sectioned tissue to elucidate the events

involved in proper pollen development. This study proposed and evaluated a protocol for

exposing developing microspores to be examined by Scanning Electron Microscopy

(SEM). Utilizing this protocol, comparative analyses of the superficial features present at

the early, middle, and late tetrad as well as at released microspore stages of the model

plants *Brassica rapa* and *Arabidopsis thaliana* were conducted. The utility of the

technique was then evaluated through the examination of three Arabidopsis pollen wall

mutants at multiple developmental stages. The *defective in exine formation 1, callose

synthase 5-2* and *thin exine 2-2* mutant lines are known to exhibit defective exine

patterning. The *dex1* mutant demonstrates abnormal sporopollenin deposition where aggregates form and coalesce randomly on the microspore surface (Paxson-Sowders et al. 1997). The *cals5-2* mutant exhibits aberrant callose synthesis at the microsporocyte stage leading to deposition of globular aggregates and improper exine formation (Dong *et al.* 2005). The *tex2-2* mutant was characterized by the presence of an extremely thin mature exine that lacks patterning (Dobritsa et al. 2011). In addition, this study aimed to further elucidate the role of DEX1 in pollen wall development through indirect immunocytochemistry of developing microsporocytes and tetrad microspores as well as understand how the distribution of this protein may differ in known pollen wall mutants. The methods developed in this study proved effective and allowed for observation of the entire surface of developing microspores with high resolution and three-dimensional qualities. These protocols provided new information in the characterization of pollen wall development in both normal and mutant plants. In addition, it revealed unique features and characteristics of sporopollenin deposition and exine development not readily observed in sectioned tissue nor explicitly described in conventional literature.

TABLE OF CONTENTS

LIST OF FIGURES

ACKNOWLEDGEMENTS

My sincerest thanks for the time and guidance of:

Dr. Heather Owen

&

Dr. Douglas Steeber and Dr. Dazhong Zhao

A special thanks to:

Alex Eisold and Katrina Olsen

Zhao Lab
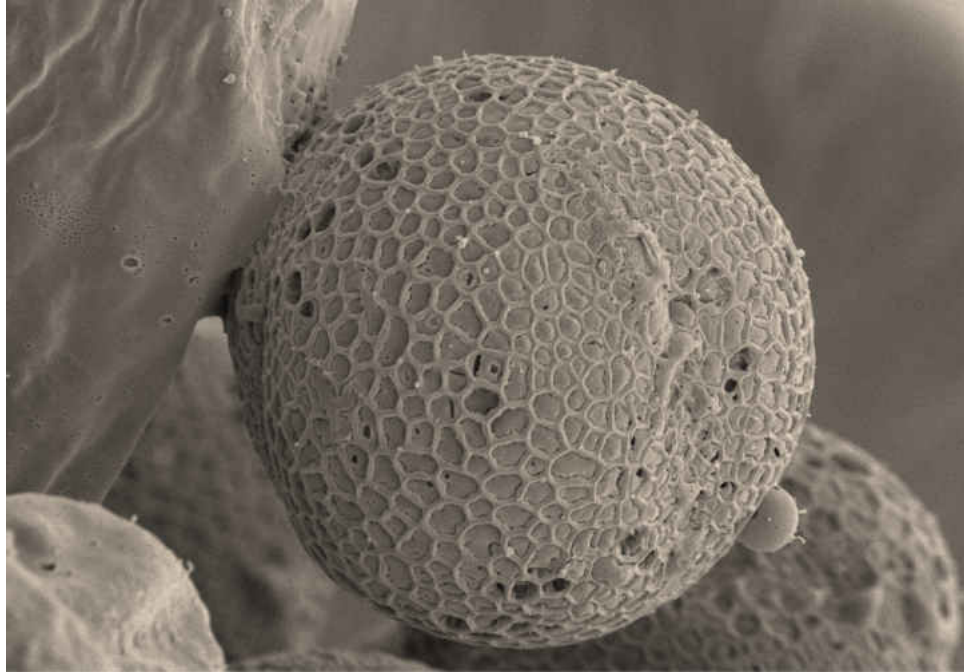
'Nature is greatest in its very smallest details' - Linnaeus

Chapter 1: Introduction to Pollen Wall Development

For decades, *Arabidopsis thaliana* has been the organism of choice for studying plant development. What makes *Arabidopsis* advantageous above all other flowering plants is the relatively short cultivation time of this organism. Additionally, it remains small in stature through adulthood, exhibits profound prolificacy and contains a small nuclear genome consisting of 5 chromosomes, the majority of which has been sequenced. These advantages promote growth within the scientific community and foster investigation into the unique organizational and physiological attributes of this organism (The Arabidopsis Genome Initiative 2000).

Despite the complexity in methods of reproduction and diversity in form, color and function, angiosperms exhibit a common architectural plan to the structure of the flower. Flowers of *Arabidopsis*, like most flowering plants, exhibit four concentric whorls, or rings, of organs (Robles and Pelaz 2005). In *Arabidopsis,* the perianth, or non-reproductive layer, of the flower consists of an outer whorl comprised of four sepals and an inner whorl of four petals. It is common for the petals to alternate with the sepals (Hill and Lord 1989). The subsequent whorl that resides to the interior of the sterile whorls is the androecium. In *Arabidopsis*, the androecium exhibits a total of six stamens, the male reproductive structure of the flower. Each stamen is comprised of an anther and a filament. Centrally located and encircled by all other floral organs is the female reproductive structure: the gynoecium (Ma 2005; Sanders *et al.* 1999).

The anther is the site of development for the male reproductive unit: the pollen grain. A mature pollen grain exhibits a protective coating called the pollen wall. This complex and multi-layered structure enhances the longevity of the gametes contained

within it by acting as a protective barrier from adverse environmental conditions such as ultra-violet light, aridity, and extreme temperatures (Jiang *et al.* 2013). In addition, the pollen wall functions as a genetic barrier by playing an essential role in the pollen selectivity during fertilization (Edlund *et al*. 2004). In *Arabidopsis*, the mature pollen wall exhibits a reticulate pattern comprised of arches called tectum and pits called lacunae. The arches are supported by rod-like structures commonly referred to as columellae or baculae (Figure 1). Residing between the sculpted intercolpal regions are three regions of modified exine called apertures. Unlike the sculpted intercolpal regions, the apertures are smooth and unpatterned. Despite vast diversity in patterning observed between species, the stratification of the pollen wall remains consistent. In general, the mature pollen wall can be divided into two distinct layers (Heslop-Harrison 1971). The outermost layer is called the exine. The exine can be further subdivided into the sculpted sexine, and a foot layer called the nexine. Residing beneath the exine is a basal layer called the intine. Prior to final maturation, the pollen wall is coated with a heterogeneous proteinaceous layer derived from the secretory system or physical breakdown of surrounding anther tissue. This covering has been termed perine, tryphine and pollenkit and is believed to provide a variety of functions ranging from adhesion to pollinators to inducing or preventing the initiation of fertilization (Heslop-Harrison 1971).

Unlike the intine, which is predominantly composed of cellulosic compounds, the primary constituent of the exine is sporopollenin. This compound imparts the physical strength and chemical inertness that allow pollen grains to survive in adverse environments for an extended period of time. The recalcitrant nature of sporopollenin is such that pollen samples have even been recovered from fossilized rock (Jones and Rowe

1999). Due to the resilient nature of the compound, the exact composition remains uncertain. Recently, biochemical assays involving Fourier Transform–Infrared (FTIR) and Nuclear Magnetic Resonance (NMR) spectroscopy propose that sporopollenin is a complex biopolymer synthesized from long fatty-acids chains (Arriizumi and Toriyama 2011; Liu and Fan 2013). In addition to the composition of sporopollenin, a second point of contention pertains to whether the sporopollenin deposited on the microspore surface at tetrad stage is the product of the surrounding anther tissue solely or forms as a result of contributions from both gametic and sporophytic tissues. Dickinson proposed that as the sporopollenin deposited at this stage is within the confines of the impervious callose wall, the sporopollenin must be a product of the microspore itself (Dickinson 1976). This sporopollenin is referred to as protosporopollenin or S-Sporopollenin. It exhibits a pliable characteristic that permits microspore expansion upon the dissolution of the callose wall. By contrast, the sporopollenin produced by the tapetum, the somatic cell layer directly adjacent to and encompassing the developing pollen, is much more rigid. This difference in stiffness between the two types may result from differences in polymerization. Dickinson suggests S-sporopollenin could be partially polymerized material and acts as a precursory component later used in the formation of T-Sporopollenin (Dickinson 1976; Liu and Fan 2013). The addition to the developing exine from the surrounding tapetum occurs regardless of the state of the developing microspore, indicating the maturation of the exine does not require the participation of the microspore (Dickinson 1976).

In Arabidopsis, pollen development begins with the pre-meiosis stage. Progenitor cells called microsporocytes reside in the very interior of the anther locule, and begin to synthesiz a specialized cell wall composed of callose. Callose, a β-1,3 glucan, is

synthesized by a class of enzymes known as callose synthases. Once encapsulated in

callose, each microsporocyte undergoes meiosis (the meiosis stage). Following meiosis,

cytokinesis ensues with the inward growth of the callose wall, leading to the production

of four individual microspores. This tetrahedral arrangement of four microspores encased

in a thick callose wall is termed a tetrad, and thus the stage at which they are formed is

commonly referred to as tetrad stage. Following the tetrad stage is the released

microspore stage where enzymes released from the surrounding tapetal cells digest away

the callose wall, releasing the microspores into the locule of the anther. Upon release, the

microspores begin to increase in size. Each microspore subsequently undergoes two

mitotic divisions to develop into a mature pollen grain (Heslop-Harrison 1971; Ariizumi

and Toriyama 2007). A general representation of development of the pollen wall at each

stage is depicted in Figure 2. In addition, the development of the pollen wall for other

species has been thoroughly described (Heslop-Harrison 1971; Blackmore *et al.* 2007;

Wallace *et al.* 2011).

Studies concerning *Arabidopsis* development have predominantly utilized

sectioned tissue in conjunction with transmission electron microscopy as a means of

elucidation of the process. To gain new insights into the mechanisms behind pollen wall

development, this study attempted to examine pollen wall development in three

dimensions using scanning electron microscopy (SEM). With this aim, two questions

were proposed; can the cell surface be exposed while preserving any features through

removal of the cell wall and preparation for SEM and will utilizing SEM depict features

not observed in sectioned tissue? The proposed protocol was assessed and utilized to

conduct a comparative analysis of the superficial features present at the early, middle,

and late tetrad as well as released microspore stages during exine development in the model systems *Brassica rapa* and *Arabidopsis thaliana*. The utility of the technique was further evaluated through the examination of three Arabidopsis pollen wall mutants at multiple developmental stages. The *defective in exine formation 1, callose synthase 5-2* and *thin exine 2-2* mutant lines are known to exhibit defective exine patterning. The dex1 mutant demonstrates abnormal sporopollenin deposition where aggregates form and coalesce randomly on the microspore surface (Paxson-Sowders et al. 1997). The *cals5-2* mutant exhibits aberrant callose synthesis at the microsporocyte stage leading to deposition of globular aggregates and improper exine formation of the mature grain (Dong *et al.* 2005). The tex2-2 mutant was characterized by the presence of an extremely thin mature exine that lacks patterning (Dobritsa et al. 2011). The timing of expression and involvement in pollen development of these genes can be observed in Figure 2. In addition, this study aimed to further elucidate the role of DEX1 in pollen wall development through indirect immunocytochemistry of developing microsporocytes and tetrad microspores as well as to understand how the distribution of this protein may differ in known pollen wall mutants.

Figure 1: Scanning electron micrographs of the exine of a mature pollen grain. (a) Mature pollen grain showing reticulate patterning and one of the three apertures (arrow) present on the grain. Size bar measures 10 μm. (b) Higher magnification of the exine. The principal exine components tectum (T) and columellae can be observed (C). Size bar (a) measures 10 μm; (b) measures 500 nm.
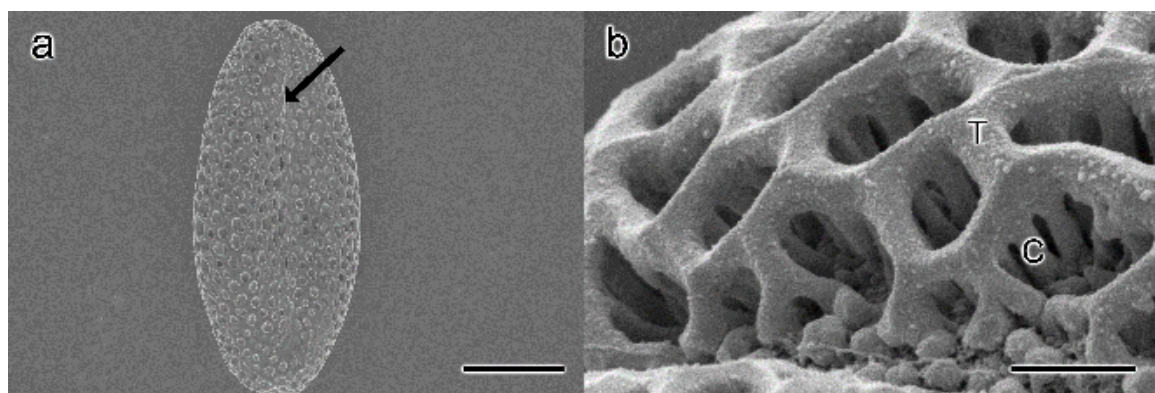
Figure 2: Diagram of wall development depicting the changes at the periphery of the microsporocyte/microspore. Bolded letters correspond to specific stages in pollen wall development. (A) Pre-meiosis. (B) Meiosis. (C) Cytokinesis. (D, E & F) Tetrad Stage. (G) Released Microspore. (H) Ring Vacuolate Microspores. Expression time and location of pollen wall genes examined in this study are represented. Not all genes essential for pollen wall development are depicted. Diagram adopted and modified from Blackmore *et al.* (2007).

Callose Wall
Formation: CALS5

Primexine and
Sporopollenin
deposition: *DEX1*

tectum

callose

bacula

A   B   C

primexine

foot layer

intine

D   E   F   G

plasma
membrane

?

cytoplasm

H

Transport of precursory
Primexine materials:
TEX2
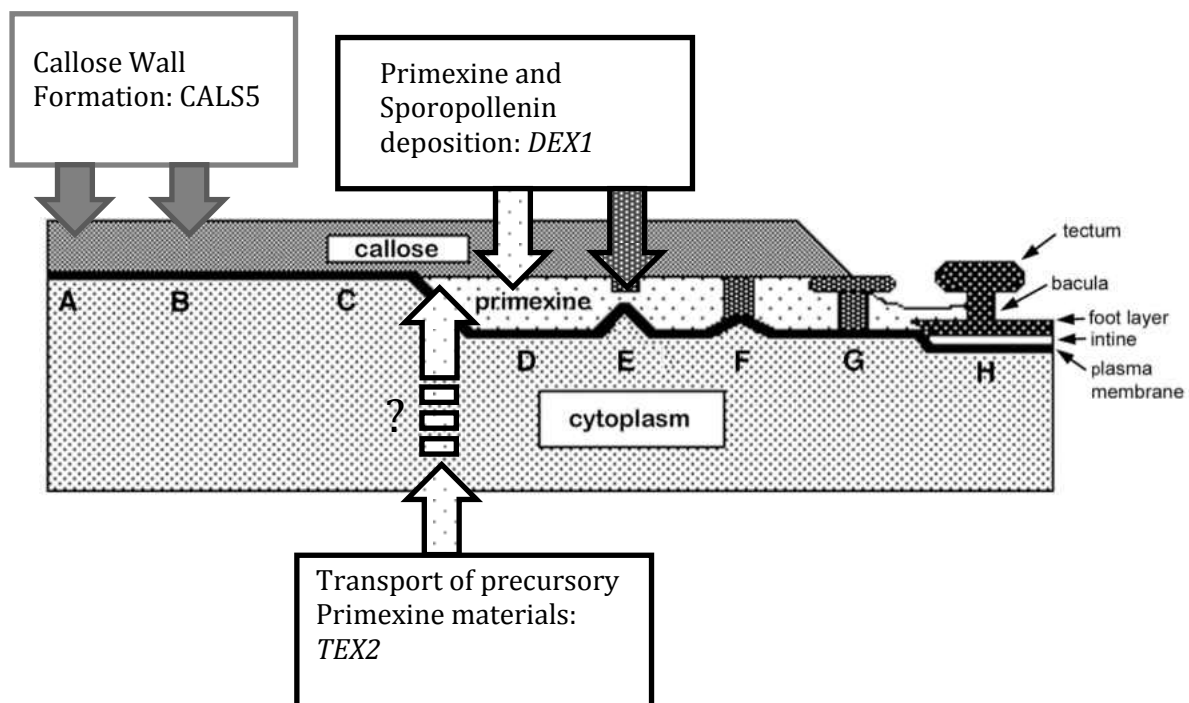
Chapter 2: Protocol Evaluation and Descriptive Analysis of Early Exine Development in *Brassica rapa*

Introduction:

The first perceivable evidence of the microspore wall appears very early in the tetrad stage. At the onset of wall development, the microspore deposits a glycoclayx-like fibrillar material called primexine matrix (Jiang *et al.* 2013). This material accumulates between the microspore membrane and the callose wall in discrete locations. Later, the plasma membrane withdraws from the sites of primexine matrix deposition, forming invaginations at regular increments. Electron dense material, presumed to be sporopollenin synthesized by the microspore, is then deposited at the crests of undulating membrane against the callose wall (Paxson-Sowders *et al.* 1997). This area, which corresponds to the tectum of the mature exine, accumulates sporopollenin first, forming the recognizable structure called protectum. Deposition continues, forming the supportive rod-like structures called procolumellae followed by the basal foot layer (Blackmore *et al. 2007*).

Following the establishment of the primexine, named for its role in establishing the mature exine as well as existing prior it, the microspores are released into the anther locule by the dissolution of the callose wall. The dissolution is facilitated by the release of callase enzymes produced from the surrounding somatic tissue called tapetum (Lersten 2004). Upon release, each microspore undergoes rapid increase in size and diameter. In *Lilium*, the microspores have been noted to increase in volume by nearly 2.8 times in only 24 hours. *Zea* species have demonstrated an even greater increase, around 1,200 times post release (Heslop-Harrison 1971; Rowley and Skvarla 2000). As the microspore

expands, sporopollenin precursor material is secreted from the tapetum, augmenting the pre-existing exine in thickness and rigidity (Dickinson 1976).

To better understand the mechanism behind pollen wall development, a protocol involving enzymatic digestion and physical force was developed and tested on the plant model *Brassica rapa*. This protocol was established to remove the enveloping callose wall while preserving underlying features present at the microspore surface in an attempt to observe how patterning may be evolving during development as a whole. We hypothesize that examining the developing microspore wall by SEM will reveal unique features and characteristics of sporopollenin and exine development not readily identifiable in sectioned tissue. Three digestion mediums were evaluated based on the aforementioned criteria at microsporocyte as well as early, middle and late tetrad developmental stages by scanning electron microscopy.

Materials and Methods:

Whole Mount Enzymatic Digest

Plant material utilized in the whole mount squash experiments consisted of anthers from *Brassica rapa* (from Carolina Biological – standard variety) flower buds. Seeds were planted directly to commercial potting mix (Sungro Metro Mix 360) and placed in a 20°C growth chamber under 16/8 hour light and dark cycle with 75% humidity conditions.

Inflorescences prior to bolting, approximately 2-3cm in height, were harvested and fixed overnight at room temperature in 3.7% paraformaldehyde, 5mM EGTA and 0.05M potassium phosphate buffer (pH 8.0) (Wick 1993). Following fixation, tissue was rinsed with 0.05M potassium phosphate buffer (pH 8.0) several times over two hours.

Inflorescences can be stored in potassium phosphate buffer for up to one month at 4°C or longer if remaining in fixative.

Coverslips coated with poly-l-lysine were prepared prior to squashing the anthers. 22 millimeter round coverslips (VWR 48282 063) were chosen due to the ease with which the substrate could be manipulated for scanning electron microscope preparation.

In this study, the desired stages of development included the microsporocyte, tetrad and released microspore stages. One anther was excised from each fixed floral bud, squashed between a microscope slide and coverslip prior to examination with a compound light microscope to determine the stage of development. When the appropriate stages of anther development were obtained, the remaining anthers from each bud were removed and squashed with moderate pressure between two poly-l-lysine coated coverslips (Peirson *et al.* 1997). The sample was allowed to dry for several minutes prior to separation of the coverslips. It is important to note the sample must not completely dry out prior to separation of the coverslips because complete drying may result in artifacts in the ultrastructure of the sample.

One coverslip from each set was then incubated with 250µl of a digestion medium, while the plant material on the other was kept under a drop of potassium phosphate buffer in lieu of the digestion medium to serve as control. Three digestion solutions were examined in this study:

- 1.4% β-glucuronidase (Sigma L2890) in 7% sucrose (Albini *et al*. 1984
- 0.3% cytohelicase (Sigma C8274), cellulase (Sigma C9422) and pectolyase (Sigma P3026) in sodium citrate buffer (pH 4.5) (Ross *et al.* 1996; Zhao *et al.* 2003).

- 0.4% (w/v) cytohelicase (Sigma C8274) in 1.5% sucrose (w/v) and 1%

  polyvinylpyrrolidone (Fischer BP431-100) (w/v) (Clapham and Ostergren 1984;

  Peirson *et al.* 1997).

 Samples were incubated in the digestion medium for a minimum of two hours at 37°C in

a glass Petri dish with wet filter paper. Upon completion of digestion, the samples were

rinsed three times with potassium phosphate buffer for 5 minutes per rinse. Excess buffer

was removed by placing a laboratory wipe at the periphery of the coverslip after each

rinsing step and care was taken to keep the plant material submerged in fluid throughout

all of the steps above, as well as those that follow (Figure 3).

Scanning Electron Microscopy Preparation and Observation

The squashed anther tissue on the coverslips was post-fixed in 1% osmium

tetroxide (OsO_4) for a minimum of 12 hours. The samples were subsequently rinsed with

double distilled water 3 times for 10 minutes per rinse before undergoing dehydration.

The water was removed from the coverslips in a manner similar to that described above.

The coverslips with the tissue were placed into a carrier (Tousimis 8767) and

moved through a graded ethanol series (20, 40, 60 80, 100%) and then once with 100%

absolute ethanol for thirty minutes at each increment for the dehydration. In order to

preserve the structural integrity of the sample, the tissue was critical point dried using a

Balzers Union CPD 020 with carbon dioxide as a transitional fluid. The coverslips were

then mounted onto 1 inch diameter specimen stubs before receiving a layer of colloidal

graphite paint at the periphery of the coverslip. The paint was dried either by placing the

mounted sample under vacuum for a minimum of 1 hour or by leaving it at room

temperature overnight in a closed container with a desiccant.

The mounted samples were then coated with 8 nanometers of iridium using an Emitech K575X sputter coater. The sample were subsequently tilted and an additional 2 nanometer layer of iridium was applied. The prepared samples were observed using a Hitachi S-4800 scanning electron microscope. Any image editing for manuscript figure construction was conducted using Photoshop v.5.5 for Windows.

Results:

Enzymatic digestion trials of the callose wall removal were conducted using *Brassica rapa* instead of *Arabidopsis thaliana* owing to the much larger *B. rapa* anthers and ease with which they could be excised from the developing floral buds (Figure 4). The three different digestion mediums were evaluated based on two criteria; 1) for effectiveness in the removal of the callose wall when compared to the control material contained on each corresponding untreated coverslip and 2) for preservation of any underlying features at the microsporocyte and microspore surface. The first trial involved digesting the sample with β-glucuronidase in 7% sucrose solution. Following incubation in the digestion medium, the callose wall remained substantially intact though the cells exhibited some superficial damage to the callose wall and appeared slightly more porous when compared to the respective control (Figure 5a-b). The second trial involved an incubation of tissue in a mixture of cytohelicase, pectolyase, and cellulose at a concentration of 0.3% each in citrate buffer. The control tissue exposed to the potassium phosphate buffer remained intact and encased in the callose wall as expected (Figure 5c). The sample incubated in the digestion medium exhibited isolated microspores and what are presumed to be coenocytic microsporocytes. No presence of the wall could be observed. However, material presumed to be cytoskeletal elements and intracellular

material was observed (Figure 5d). The third trial involved incubation of tissue in 0.4%

cytohelicase in 1.5% sucrose and 1% polyvinylpyrrolidone (PVP). Control tissue

remained in the callose wall (Figure 5e). The tissue samples incubated in cytohelicase

only exhibited isolated microspores that were free of the callose. Features presumed to be

tectum and apertures were readily apparent. The surface features appeared intact despite

the enzymatic digestion, and subsequent preparation for the SEM (Figure 5f).

Since only the cytohelicase in sucrose and PVP treatment was found to be

effective at removing the callose wall without damaging the surfaces of the cells

contained therein, it was subsequently used to prepare additional material at alternate

developmental stages so that a developmental series of images could be acquired and

assessed. Microsporocytes prior to cytokinesis retained a distinct angularity, an indicator

of the presence of the wall (Figure 6a). Microsporocytes in the process of cytokinesis

were cleanly severed from the surrounding callose wall. The surface appeared non-

distinct and smooth. Large invaginations in the surface, presumably cleavage furrows,

were observed. Several pores orientated linearly along the trough of the cleavage furrow

could also be discerned. The pores were believed to be openings associated with

convoluted sheets in post meiotic callose deposition and cytokinesis (Otegui and

Staehelin 2004). The four lobes of the future microspores were also observed (Figure 6b).

The tetrad stage was divided into three stages. The labels used include young, middle and

late tetrad as initially described by Gabarayeva *et al.* (2009). Microspores defined as

'young tetrad' were defined by the smooth surface and a lack of any cell coating

(Gabarayeva *et al.* 2009). Young tetrad microspores observed in this study also exhibited

a relatively smooth, nondescript surface. Additionally, microspores of this stage

demonstrated a distinct angularity (Figure 6b). In rare instances, the young microspores

remained in the tetrahedral orientation despite removal of the callose. By the completion

of the early tetrad stage, the plasma membrane is periodically indented with shallow

invaginations (Figure 6c). At the next stage described by Gabarayeva *et al.,* termed

middle tetrad stage, the procolumellae are observed on the top of the invagination sites of

the plasmalemma, appearing as aggregates of radially oriented electron dense material

(Gabarayeva *et al.* 2009). Microspores observed at this stage exhibited consistent

features. Small, isolated clusters of material appear to collect on the ridges of the

microspore surface (Figure 6d). As development advances, deposition of this material

continues until one cohesive structure is observed residing on the ridges (Figure 6e). With

the onset of the late tetrad stage, procolumellae exhibiting a distinct form and shape are

present at the plasma membrane. Further deposition causes the procolumellae to elongate

and expand as well as the protectum arches to form and thicken. This stage in

development culminates with the presence of the fundamental exine structure and

patterning of the developing grain (Paxson-Sowders *et al.* 1997). The patterned regions

and apertures were readily apparent on the late tetrad microspores. The apertures

appeared to occupy a significant portion of the microspore surface. Through sample

orientation manipulation, procolumella could be observed residing beneath the tectum.

The overall patterning appears consistent with that of a mature pollen grain, though

highly compressed. Following the degradation of the callose wall and release into the

anther locule, the microspores begin to expand. Sporopollenin deposition from the

tapetum then takes place, causing the structures comprising the sexine to become more

prominent. The patterning observed is more readily identifiable with that exhibited by a mature grain as observed in Figure 6f (Paxson-Sowders *et al.* 1997).

Discussion:

In this study, it was demonstrated that the combination of physical force and enzymatic digestion is sufficient to release the developing microspores from the surrounding anther tissue and separate them from the enveloping callose cell wall. The means of separation employed was gentle enough to preserve the underlying structures of the microspore surface in *Brassica rapa*. The features described in this study appeared consistent with observations discussed in previous studies (Takahashi and Skvarla 1991; Paxson-Sowders *et al.* 1997; Gabarayeva *et al.* 2009).

In several instances, the squashing of anther tissue during whole mount preparation forced either a portion of or entire microspores from the callose prior to enzymatic digestion. The compression of the excised microspore against the coverslip caused a distinct deformation pattern in the exposed portions of the developing exine. Areas that experienced deformation exhibited a stretched appearance, while unaffected areas, presumed to have been constrained by the residual callose until it was digested away, remained tightly compacted (Figure 7a). Examination of such microspores through specimen orientation manipulation revealed that the two pattern types, stretched and compact, were continuous (Figure 7b-c). The squashing and consequential stretching of the microspore surface demonstrates an innate elasticity to the proexine. This corroborates with the findings of Banerjee, Rowley and Alessio validating the speculations by Beer that the principal features of the exine patterning are determined early by the isolated microspore (Heslop-Harrison 1976). Any subsequent changes to the

sexine post release may result from the volume increase during later developmental stages (Takahashi 1980). Additionally in this study, the expansion of the exine of released microspores appears to be restricted to the intercolpal regions between apertures. The apertures themselves show marginal, if any, increase in area as the microspore volume increases. A comparison of late tetrad stage microspores with mature pollen grains (Figure 8) qualitatively demonstrates this as the apertures make up a larger proportion of the late tetrad microspore surface compared to those present following callose degeneration and microspore release.

Upon closer examination by SEM, the developing exine appears to be comprised of a material that is rounded and semi-spherical in construction (Figure 9). According to Hemsley (2005), the presence of these types of structures, amusingly referred to as raspberries and muffins, reveals a great deal about the inherent properties and the environment in which this material was synthesized. In *Exine development: the importance of looking through a colloid chemistry ''window''*, Hemsley *et al*. explain the role of high molecular weight substances like glycoproteins and lipopolysaccharides in micelle formation. It is further explained that the behavior of the various micelle constructs (spherical, neat and cylindrical) may respond differently to different environmental conditions, resulting in the patterns and structures observed in the exine (Hemsley and Gabarayeva 2005).

Figure 3: General schematic of whole mount squash preparation. Diagram depicting the general steps involved in the whole mount squash technique and preparation for SEM observation.
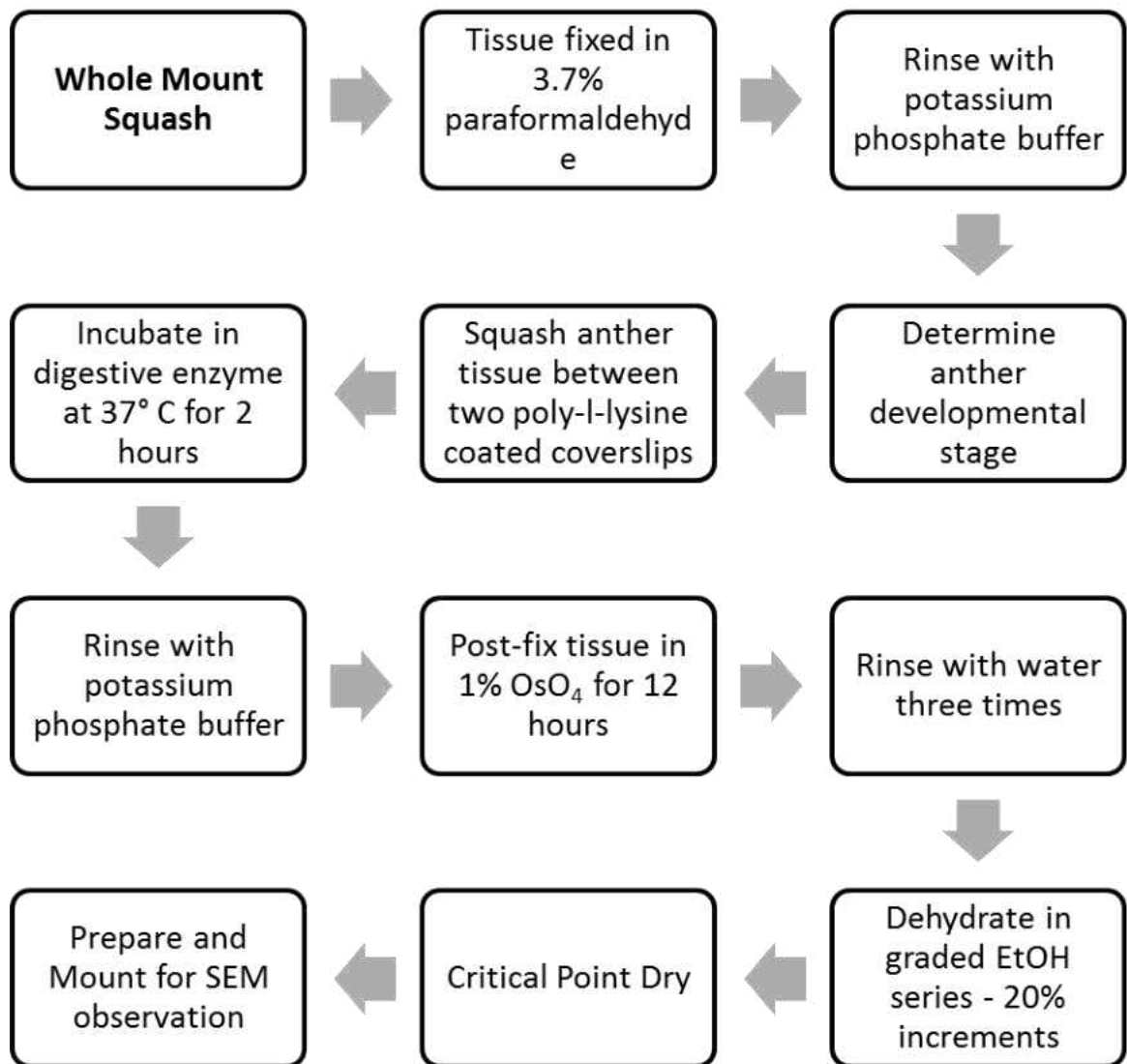
```
┌─────────────────┐      ┌─────────────────┐      ┌─────────────────┐
│  Whole Mount    │  ►   │  Tissue fixed in│  ►   │   Rinse with    │
│     Squash      │      │      3.7%       │      │    potassium    │
│                 │      │ paraformaldehyd │      │ phosphate buffer│
│                 │      │        e        │      │                 │
└─────────────────┘      └─────────────────┘      └─────────────────┘
                                                            │
                                                            ▼
┌─────────────────┐      ┌─────────────────┐      ┌─────────────────┐
│   Incubate in   │      │  Squash anther  │      │    Determine    │
│ digestive enzyme│  ◄   │ tissue between  │  ◄   │     anther      │
│  at 37° C for 2 │      │ two poly-l-lysine│     │  developmental  │
│      hours      │      │ coated coverslips│     │     stage       │
└─────────────────┘      └─────────────────┘      └─────────────────┘
         │
         ▼
┌─────────────────┐      ┌─────────────────┐      ┌─────────────────┐
│   Rinse with    │      │ Post-fix tissue in│    │ Rinse with water│
│    potassium    │  ►   │  1% OsO₄ for 12 │  ►   │   three times   │
│ phosphate buffer│      │      hours      │      │                 │
└─────────────────┘      └─────────────────┘      └─────────────────┘
                                                            │
                                                            ▼
┌─────────────────┐      ┌─────────────────┐      ┌─────────────────┐
│   Prepare and   │      │                 │      │  Dehydrate in   │
│  Mount for SEM  │  ◄   │ Critical Point Dry│  ◄  │   graded EtOH   │
│   observation   │      │                 │      │  series - 20%   │
│                 │      │                 │      │   increments    │
└─────────────────┘      └─────────────────┘      └─────────────────┘
```

Flowchart:

Whole Mount Squash → Tissue fixed in 3.7% paraformaldehyde → Rinse with potassium phosphate buffer → Determine anther developmental stage → Squash anther tissue between two poly-l-lysine coated coverslips → Incubate in digestive enzyme at 37° C for 2 hours → Rinse with potassium phosphate buffer → Post-fix tissue in 1% OsO_4 for 12 hours → Rinse with water three times → Dehydrate in graded EtOH series - 20% increments → Critical Point Dry → Prepare and Mount for SEM observation

Figure 4: Mature *Brassica rapa* (a) and *Arabidopsis thaliana* (b) flowers. Images depicting distinct size difference in floral organs between the two species. Magnification is consistent between the two images. Size bars measure 2 mm.
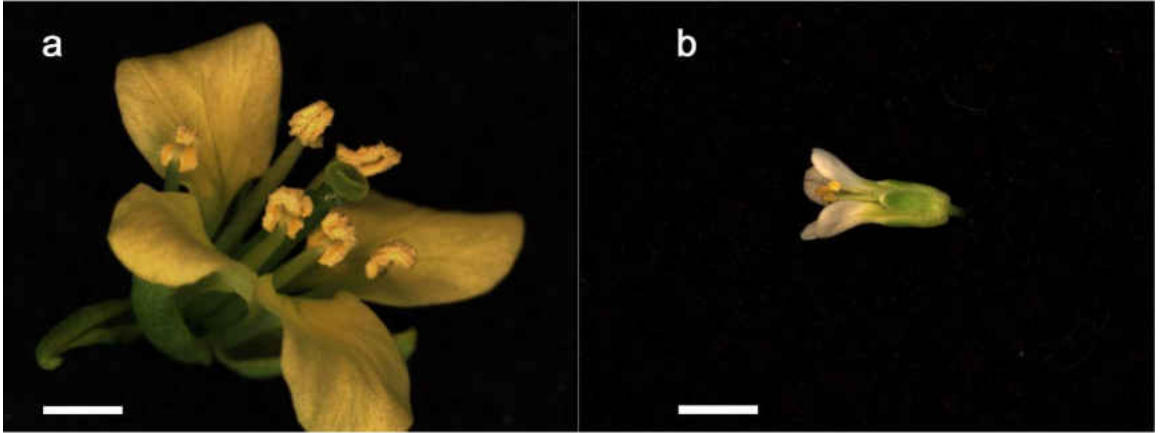
Figure 5: Enzymatic digestion experimentation with *Brassica rapa* anther tissue. (a, c, e) Control anther tissue exposed to potassium phosphate buffer. (b) Tissue digested with β-glucuronidase. (d) Tissue digested with cytohelicase, pectolyase and cellulose mixture. (f) Tissue digested with cytohelicase in sucrose and polyvinylpyrrolidone solution. Size bars measure 2 μm.
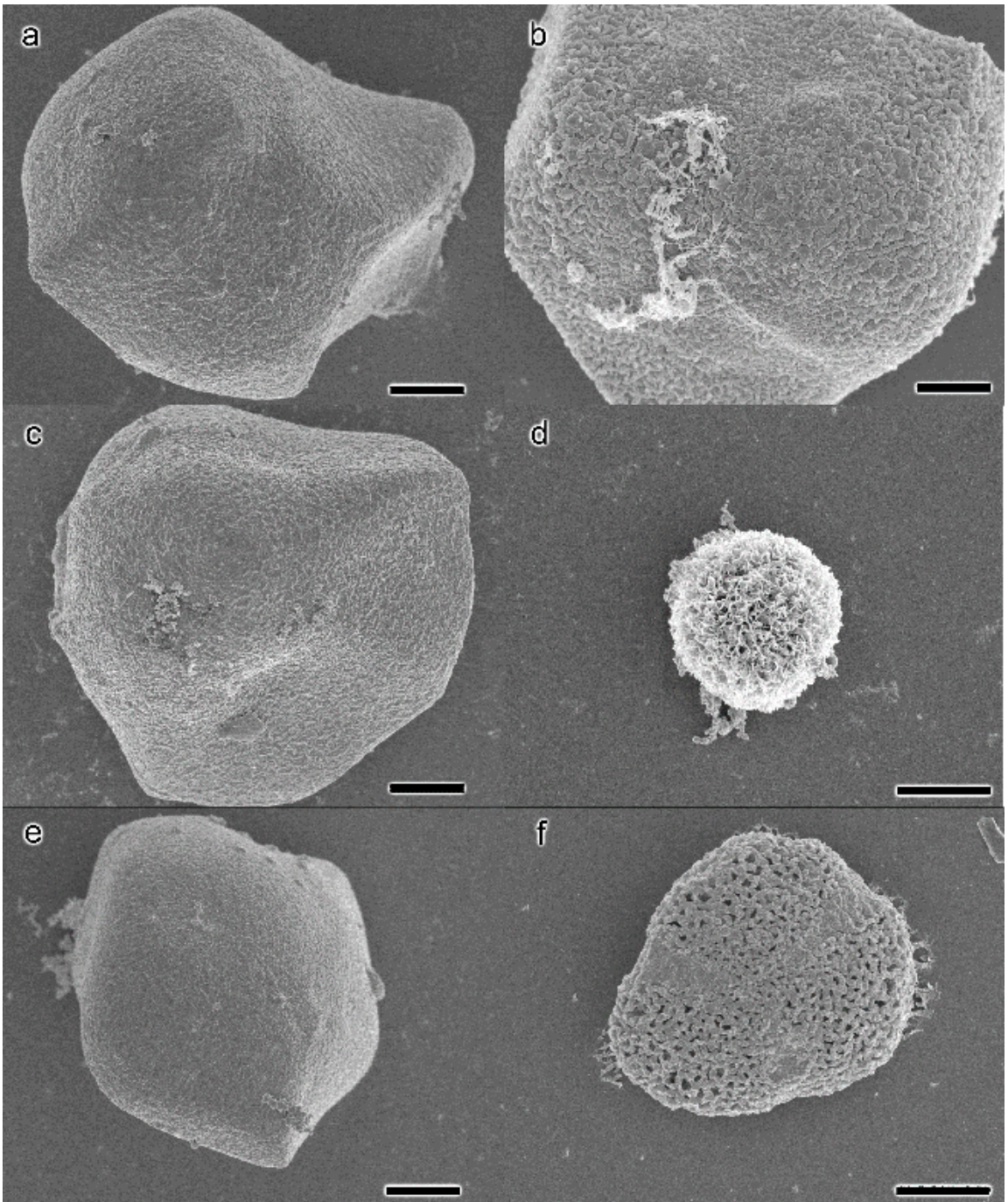
Figure 6: *Brassica rapa* early pollen developmental series. (a) Microsporocytes encased in callose wall. Tissue did not receive digestion treatment. All subsequent depict digested samples. (b) Coenocytic microsporocyte free of callose wall. The four lobes of the future microspores were present. (c) Middle tetrad stage microspore with periodic and regular indentation of the plasma membrane. (d) Middle tetrad microspore with small aggregates on the ridges. (e) Late tetrad microspore with a single cohesive structure on the ridges. Latticed patterning was recognizable. (f) Late tetrad microspore prior to release. The tectum and apertures were readily apparent. The overall patterning appears consistent with that of a mature pollen grain. Size bars (a) measure 5 μm; (b-f) measure 2 μm.
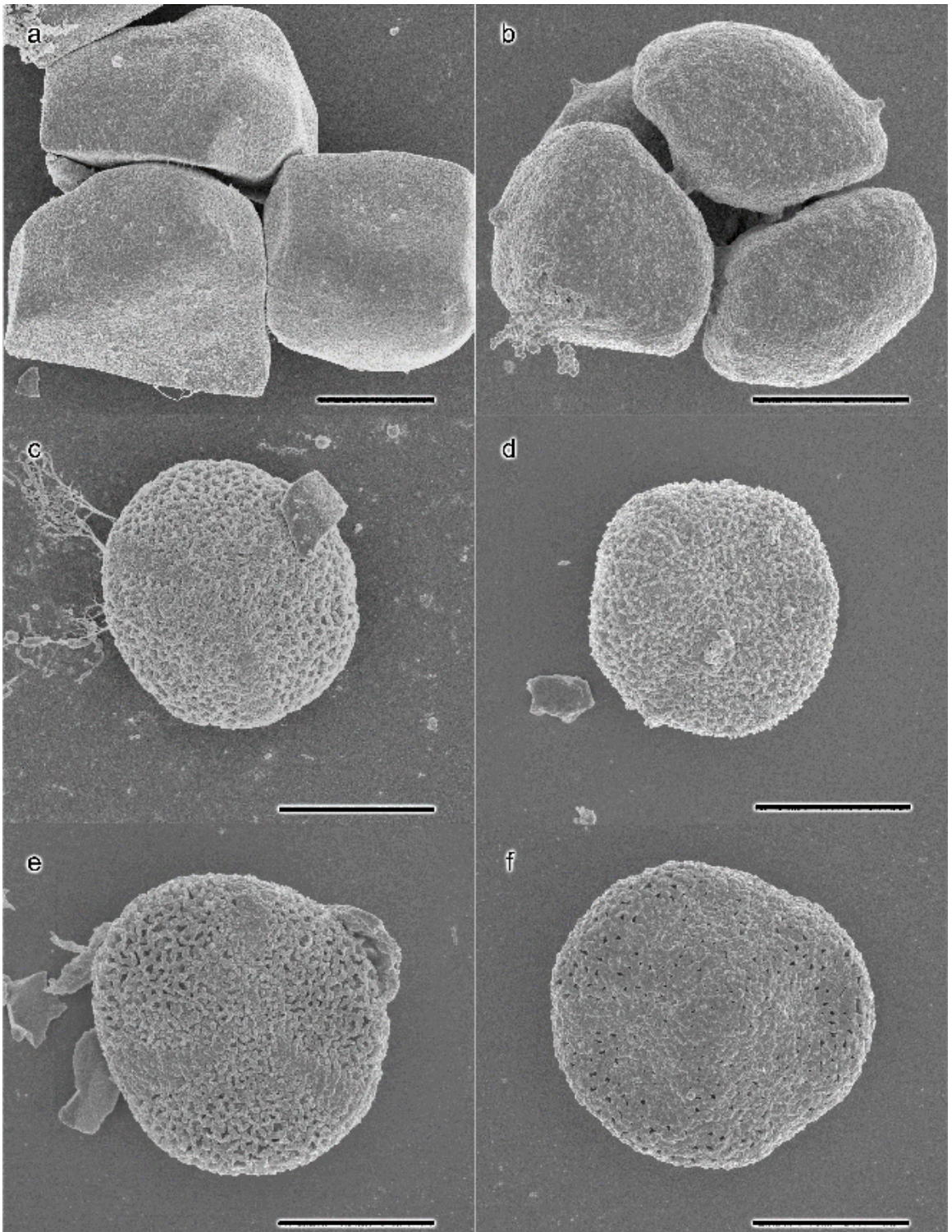
Figure 7: Squashed microspores depicting elastic nature of developing exine. (a) Late tetrad microspore depicting two distinct exine pattern types; compact and stretched. (b) The same microspore at higher magnification depicting continuity between two pattern types. (c) Alternative microspore exhibiting same stretching phenomenon. Size bars measure 2 µm.
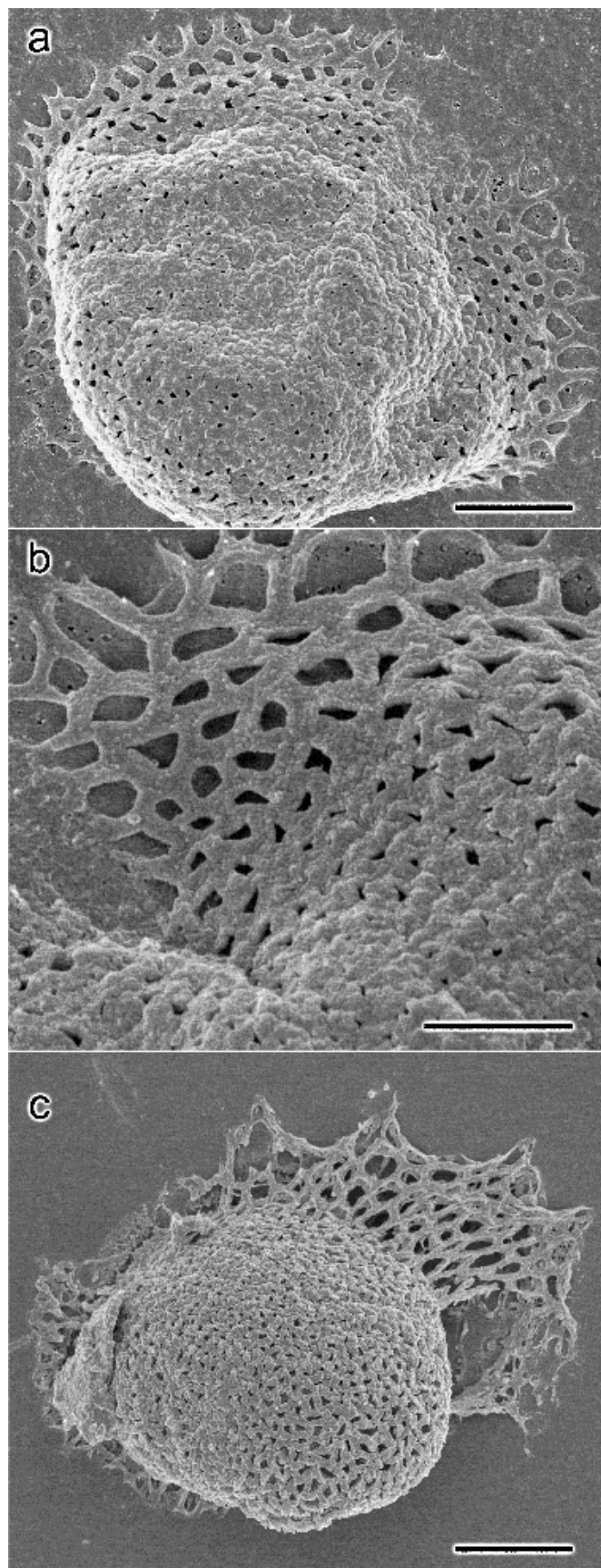
Figure 8: Comparative analysis of late tetrad stage microspores to mature pollen grains of *Brassica rapa*. (a) Late tetrad microspore exposed through enzymatic digestion. (b) Mature pollen grain. The micrographs were taken at a consistent magnification and working distance. Size bars measure 2 μm
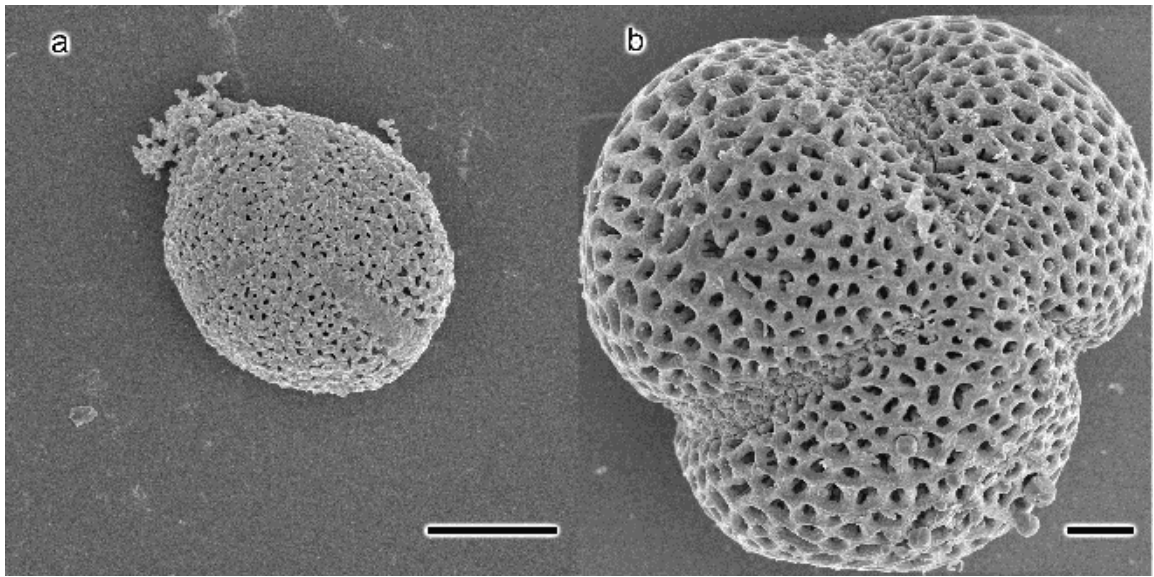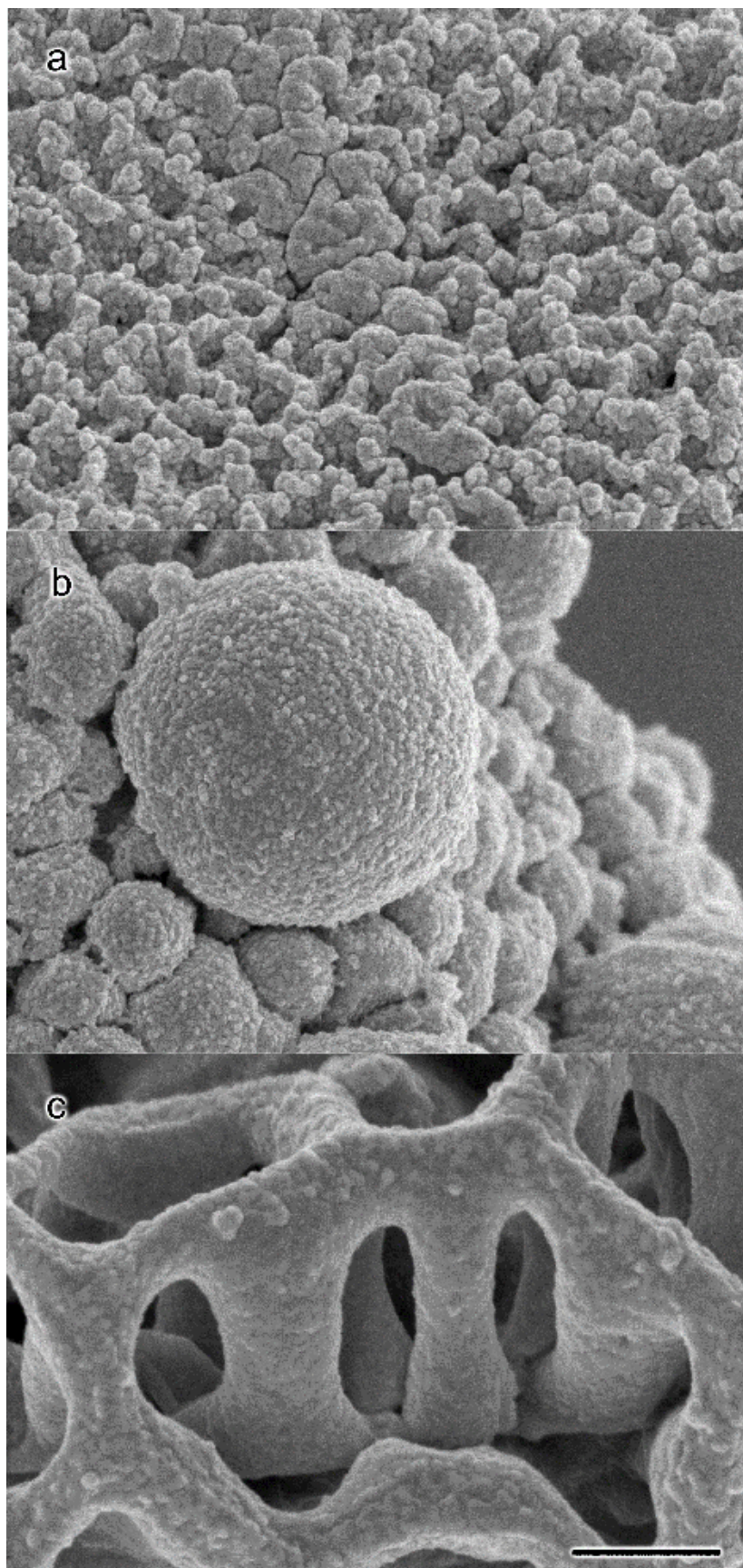
Figure 9: Proexine exhibiting construction comprising rounded and semi-spherical material. (a) Early exine and aperture on a middle tetrad stage microspore. (b) Sporopollenin aggregate of *dex1* mutant. (c) Pollen wall of a mature grain. The micrographs were taken at a consistent magnification and working distance. Size bar measures 1 μm.

Chapter 3: Harmomegathy, Pollen Expansion and Acetolysis

Introduction:

Development of the pollen grain culminates with anthesis, when the pollen grains are released from the anther locules into the surrounding environment. To survive in the new arid setting, pollen undergo a phenomenon called harmomegathy. Harmomegathy describes the characteristic folding of the pollen grain to adjust to the loss of water during dehydration. It is common for mono and tricolpate pollen grains to collapse along the aperture regions during this process. This is primarily due to the elastic and relatively thin nature of the exine at the aperture relative to intercolpal regions of the pollen wall. As indicated previously, the pollen wall is composed of two distinctive layers. The outer sculpted layer, referred to as the exine, is rigid, chemically recalcitrant and remains relatively unchanged during the expansion or collapse of the pollen grain. The basal intine, however, is predominantly cellulosic in composition and much more permeable to the movement of water. To prevent excessive desiccation following release, the pollen grain collapses and folds upon itself, leaving only the thick and impermeable exine exposed (Volkova *et al.* 2013).

Paradoxically, studies examining the exine of mature grains have found it to be both flexible and elastic as well as rigid. Rowley *et al.* conducted compression experiments on acetolyzed mature grains from a variety of genera. These mature grains were frozen in buffer and then forced through a small aperture in a cylinder. The results were equated to a fractured tennis ball. The compressed grains showed large fractures, but the remaining wall exhibits enough elasticity to 'snap' back to a nearly intact appearance (Rowley and Skvarla 2000). Additionally, the sporopollenin present at the

release of the microspore from the callose wall demonstrates an innate elasticity. Upon

dissolution of the callose, the vacuoles present within the microspores begin the process

of water absorption and swell. This leads to a rapid increase in diameter. Lily

microspores, for example, exhibit a 2.8 times increase within the first 24 hours following

microspore release. Studies conducted on *Sparangium androcladium* found the diameter

of the microspore to double once freed in the pollen sac (locule). During the same period,

it was estimated that the expansion resulted in a reduction of thickness of the exine layers

by as much as 75% (Heslop-Harisson 1971; Lertsen 2004), clearly demonstrating the

capacity of exine to stretch.

A common means of isolating and studying pollen wall morphology involves a

method called acetolysis. First introduced by G. Erdtman, acetolysis is a ubiquitous

technique utilized by palynologists and paleobotanists alike. This process subjects the

biological material to caustic substances such as sulfuric acid, hydrochloric acid, and

acetic anhydride as well as temperatures at and near boiling. In so doing, all but the most

resilient plant material, such as sporopollenin and lignin, is stripped away. As the exine

of a pollen grain is almost exclusively sporopollenin, this is an elegant and simple means

of exposing features residing in the outer pollen wall (Hesse and Waha1987). The origin

of the exine remains a topic of great debate. The long established notion regards the

callose wall as a barrier to any synthesized materials, and thus any material deposited on

the microspore surface at the tetrad stage must be a provided by the microspore itself.

Various studies, however, have contested this view, citing that mutants exhibiting

abnormalities in primexine construction lack any problems in wall construction in the

heterozygous lines, indicating a sporophytic contribution to primexine development (Dickinson 1976).

In this study, microspores at various stages in development were subjected to the acetolysis process in an attempt to elucidate if the material being deposited during tetrad stage can be classified as sporopollenin and specifically when and where deposition takes place. Additionally, acetolyzed mature grains were subjected to drying and rehydrating treatments to access whether the elasticity of the mature sporopollenin is a function of the expanding protoplast or of the sporopollenin itself.

Materials and Methods:

Gravity Acetolysis

Conventional acetolysis utilizes centrifugation to pellet the sample between steps (Hesse and Waha 1987). Due to the fragile nature of the developing microspores, all centrifugation steps were replaced with gravity settling. The settling procedure was established based on the Utermöhl method and a modified protocol for counting algal samples as described by Paxinos and Mitchell (2000)**.** The modified acetolysis protocol established in this study is as follows:

Freshly harvested anthers of *Brassica rapa* were placed in a 3 dram shell vial containing 1 mL of 5% potassium hydroxide (w/v). The tube was incubated at 80°C for ten minutes, stirred every two minutes. Following incubation, the contents were diluted with water and allowed to settle for a minimum of twenty-four hours. The excess liquid was siphoned off, leaving enough residual liquid to cover the sample before washing the sample with 30% concentrated hydrochloric acid for 5 minutes. Water was added to the tube and the contents allowed to settle. Following the removal of excess liquid, the

sample was washed with 1 mL glacial acetic acid for 5 minutes, diluted and allowed to

settle. The sample was incubated in 1 mL acetolysis mixture (90% acetic anhydride; 10%

sulfuric acid) at 100°C for eight minutes, stirred every two minutes. Tubes were removed

from the water bath, the contents diluted and allowed to settle. The sample was washed

one final time with 1 mL glacial acetic acid for 2 minutes and stored in any residual fluid.

Fluid containing acetolyzed sample was aliquot onto silicon wafers (Ted Pella

16008) first coated with poly-l-lysine according to the method described in Chapter 2,

and allowed to settle for one hour in a glass Petri dish with wet filter paper. The samples

were dehydrated, mounted, critical point dried and sputter coated in a manner similar to

that previously described before being viewed with a Hitachi S-4800 scanning electron

microscope.

Acetolyzed Mature Grain Rehydration

Fresh anthers of *Brassica rapa* were harvested just prior to dehiscence. Any

anthers not immediately used were stored in concentrated glacial acetic acid. Long term

storage in the glacial acetic acid did not appear to adversely affect the final results. Once

collected, the anthers were subjected to the acetolysis protocol as described above. In

place of gravity settling, however, the samples underwent centrifugation at 8,000 to

10,000 rpm for 2 – 3 minutes to shorten the protocol. The resulting fluid containing the

acetolyzed pollen grains was aliquoted onto silicon wafers coated with poly-l-lysine. The

samples were then split into two treatment groups. Group one was allowed to fully air dry

overnight. Group two was dehydrated in a graded ethanol series and critical point dried.

Once dried, small subsets of these two groups were then rehydrated in water overnight.

The rehydrated group was further subdivided. One treatment group was subsequently

allowed to air dry. The second was dehydrated with ethanol and critical point dried. The final groupings of samples based on treatment were as follows: 1) air dried only, 2) critical point dried only, 3) air dried, rehydrated, and air dried, 4) critical point dried, rehydrated and air dried, 5) air dried, rehydrated and critical point dried, 6) critical point dried, rehydrated and critical point dried.

Results:

After several trials, it became apparent that microspores at the tetrad stage could not survive the rigor of centrifugation that conventional acetolysis employs. These microspores were consistently observed in a flattened state with the apertures completely missing. Even the released microspores, with a slightly more robust sexine layer, had a tendency to collapse. Only when the deposition of sporopollenin was complete and the exine matured could the pollen wall survive the acetolysis procedure involving centrifugation (Figure 10a-b).

To reduce the stress applied to the microspores, the samples were allowed to settle out by means of gravity in lieu of centrifugation. Samples exposed to gravity settling retained a distinctive three dimensional appearance. Microspores in earlier stages of tetrad development, as indicated by the thin columellae and fragmented nexine, retained their three dimensionality but consistently lacked material in the aperture regions (Figure 10c-d). Microspores that had progressed further in development however, as far as late tetrad stage, retained their physical form and material on the aperture regions (Figure 11).

Acetolyzed mature pollen grains were obtained using conventional acetolysis and then subjected to treatments involving air and critical point drying in conjunction with rehydration in water. The utilization of acetolyzed material enabled the isolation of the

pollen exine from the underlying gametophyte. By separating the two constituents, we attempted to elucidate whether the driving force behind the harmomegathy was the underlying protoplast or the pollen wall itself. Despite the varied treatments, the acetolyzed material persisted in the state following the initial drying treatment. The mature grains that were initially air-dried remained collapsed while the critical point dried material retained a spheroidal shape (Figure 12).

Discussion:

The acetolysis method, established by Erdman and expounded by Hesse, was employed in this experiment to isolate sporopollenin material from extraneous anther tissue. Sporopollenin, a highly recalcitrant material, is capable of withstanding the harsh physical and chemical treatments involved in the acetolysis method. In this fashion, any remaining material observed following the acetolysis protocol retains a high probability of being sporopollenin. The sexine structures, including apertures, were present at the late tetrad microspore stage following the acetolysis process. This suggests the material present on the intercolpal and apertural regions is likely sporopollenin. Presence of sporopollenin on the aperture regions at tetrad stage is not altogether unexpected. Studies conducted on *Nicotiana tabacum* using fluorescence and transmission electron microscopy expressed findings of phenylpropanoid sporopollenin component accumulation at aperture and exine regions in the later stages of tetrad development. Accumulation was noticeable starting at the middle tetrad stage (Matveyeva *et al.* 2012).

The mature pollen wall, once separated from the underlying protoplast, was found to retain the shape established by the initial drying step. Despite attempts at rehydration, collapsed grains that were air dried remained so while the critical point dried material

retained its three-dimensionality. This suggests the expansion and folding observed as a result of harmomegathy must be driven by the underlying protoplast or intine layer and not by the exine.

Inferior to the sexine in the pollen wall is a basal lamina called the nexine. This layer, like the sexine, is presumed to be composed of sporopollenin. In angiosperms, and in particular in *Arabidopsis,* the literature commonly places nexine formation following the dissolution of the callose wall and release of the microspore into the anther locule (Wallace *et al.* 2011; Zhou *et al.* 2015). In this study, however, the acetolysis method made apparent the presence of a developing nexine at tetrad stage, were fragments or islands of nexine observed on late tetrad microspores. It was not until after the microspore was released from the callose and began to expand that a cohesive basal layer formed (Figure 13). This seems to suggest the initiation of nexine deposition may occur earlier than previously speculated, at least in *Brassica rapa*, but does not become a contiguous layer until additional material from the tapetum is deposited. Owing to the onerous task of isolating anthers, however, the acetolysis method was not conducted on tetrad stage *Arabidopsis* anthers. The confirmation of this find will be left to future interested parties with greater patience and vision than I.

Figure 10: Acetolyzed late tetrad and mature grains of *B. rapa* by means of conventional and gravity settling methods. (a) Late tetrad microspore exhibiting compression after conventional acetolysis. (b) Mature grain exhibiting distinct spherical shape after conventional acetolysis. (c) Late tetrad microspores exhibiting compression after conventional acetolysis. (d) Tetrad microspores exhibiting 3-dimensionality after gravity acetolysis. Apertures were absent. Size bar measures 5 μm for all micrographs.
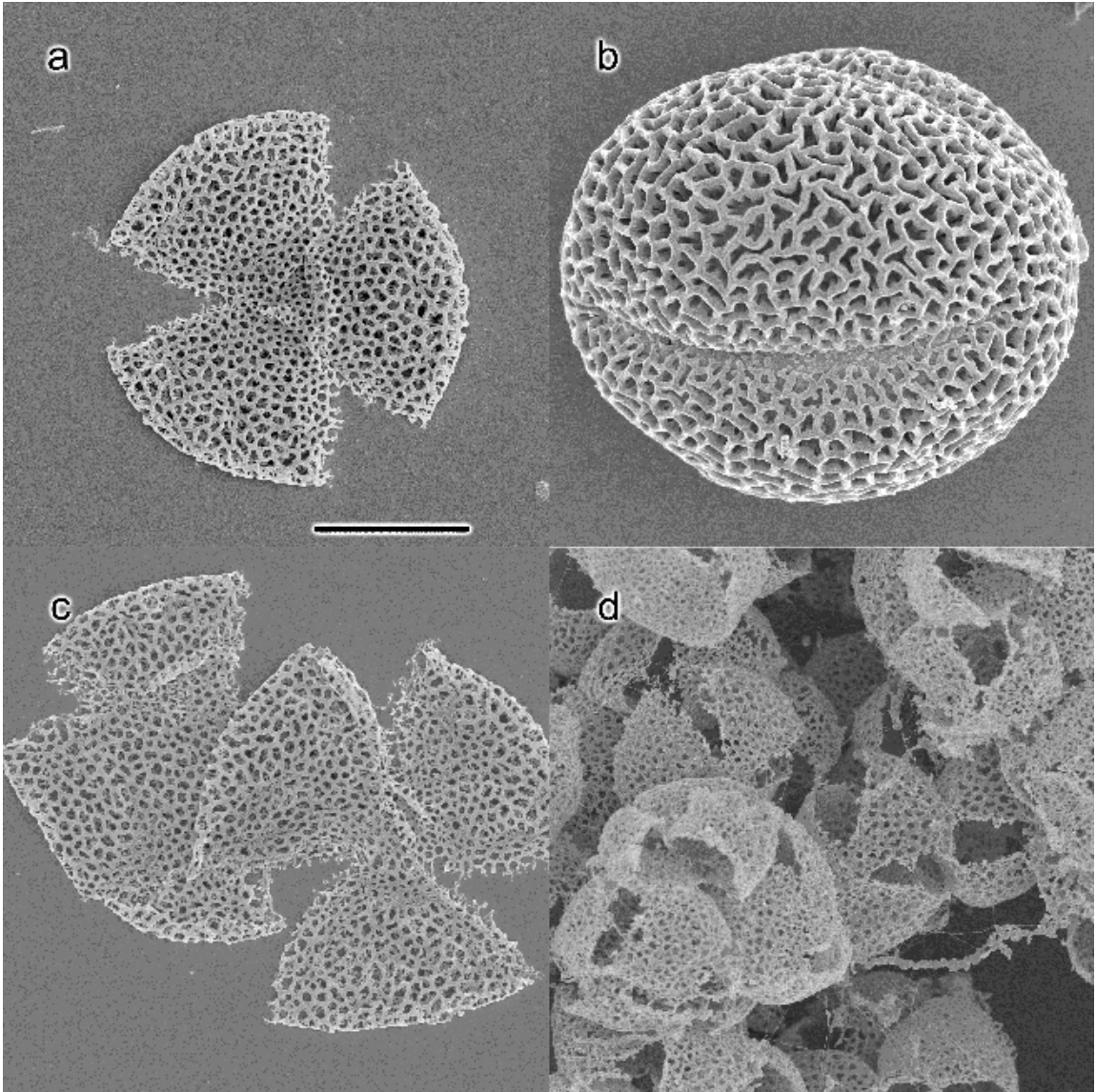
Figure 11: Gravity settled acetolyzed microspores of *B. rapa* demonstrating aperture presence. (a) Late tetrad microspores with apertures intact. (b) Higher magnification of the aperture region of the aforementioned microspore. (c) High magnification of the aperture region of alternative microspore. Size bar measures (a) 2 µm; (b-c) 500nm.
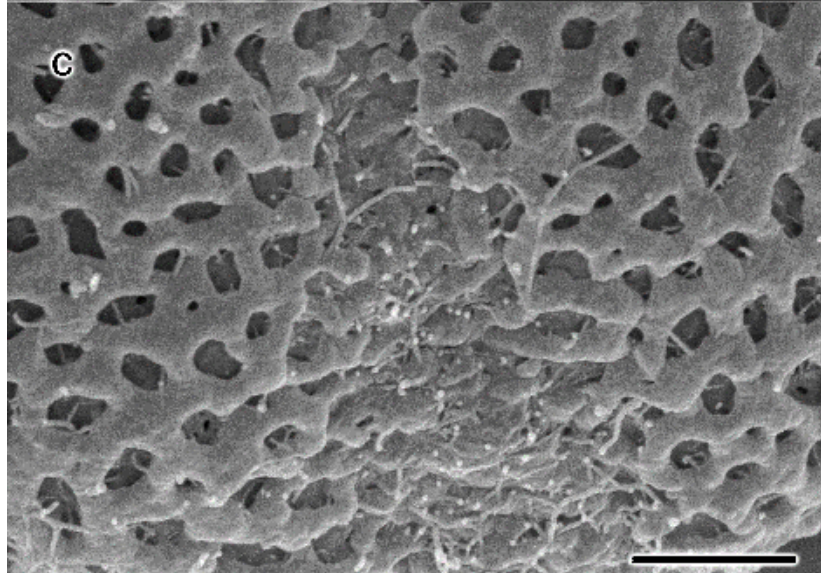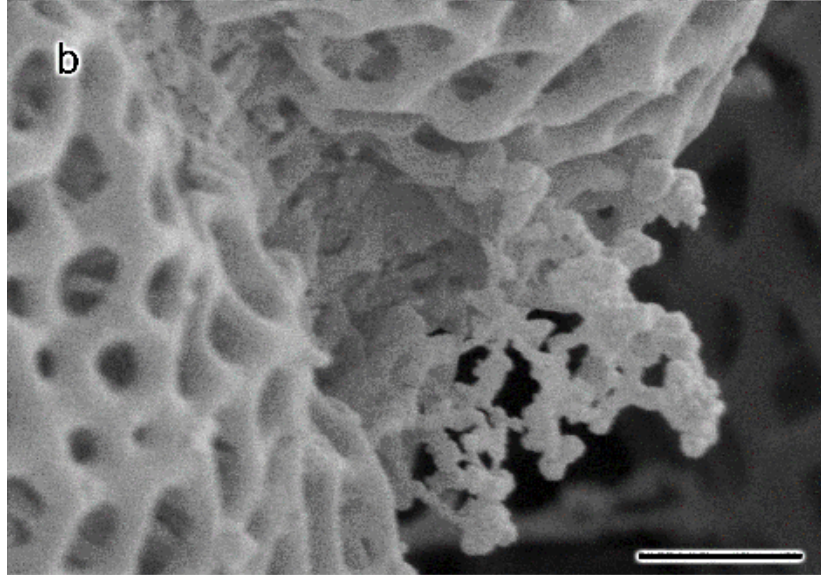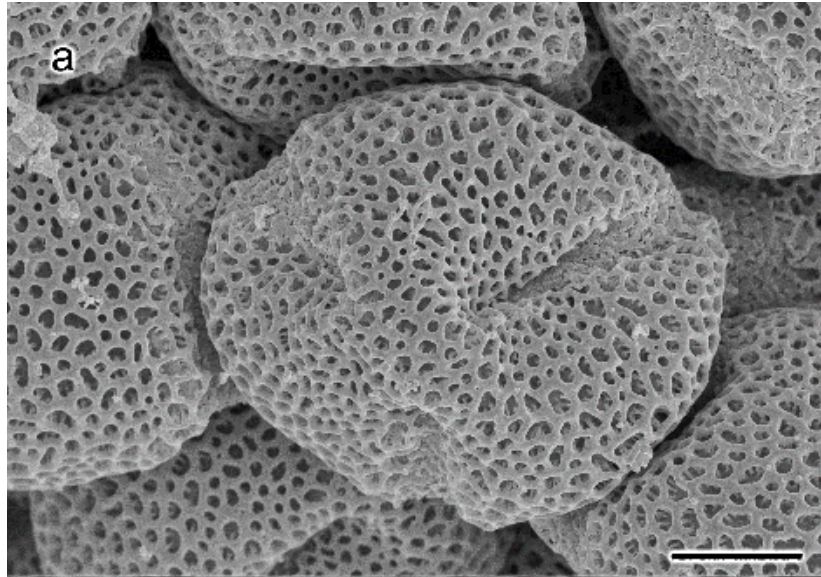
Figure 12: Comparative analysis of air dried and critical point dried acetolyzed mature grains of *B. rapa*. (a) Acetolyzed mature grain allowed to air dry. (b) Acetolyzed mature grain critical point dried. (c) Acetolyzed mature grain allowed to air dry following the initial air drying and rehydration. (d) Acetolyzed mature grain critical point dried following the initial critical point drying and rehydration. (e) Acetolyzed mature grain critical point dried following the initial air drying and rehydration. (f) Acetolyzed mature grain allowed to air dry following the initial critical point drying and rehydration. Size bar measures 5 μm for all micrographs.
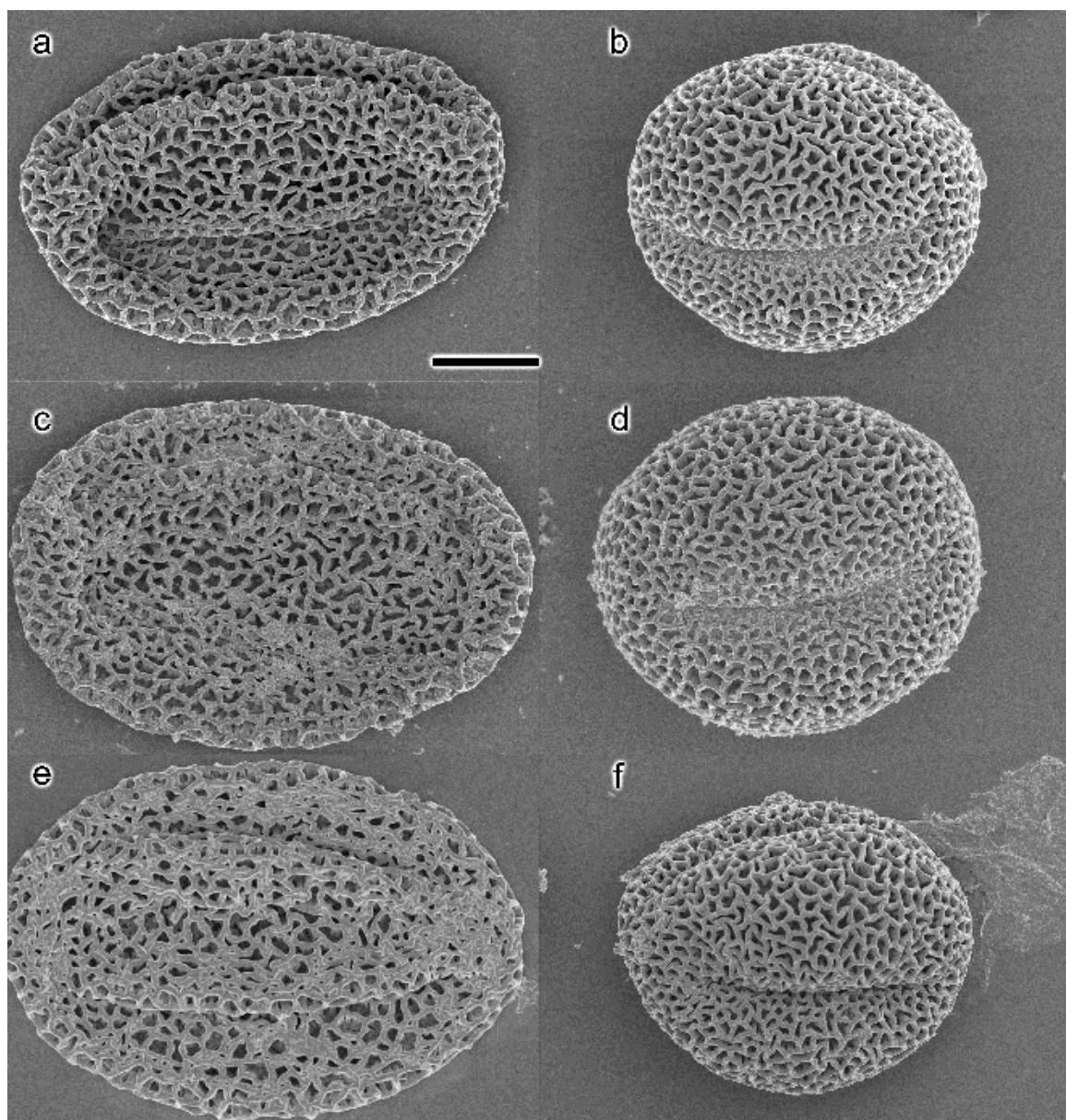
Figure 13: Presence of basal nexine on acetolyzed tetrad stage microspores. (a) Acetolyzed late tetrad microspore of *B. rapa* depicting incomplete nexine. (b) Alternate acetolyzed late tetrad microspore demonstrating a contiguous basal nexine. (c) Alternate acetolyzed late tetrad microspore under tilt to differentiate sexine from developing nexine. Micrographs were taken at a consistent magnification. Size bar measures 1 μm for all micrographs.
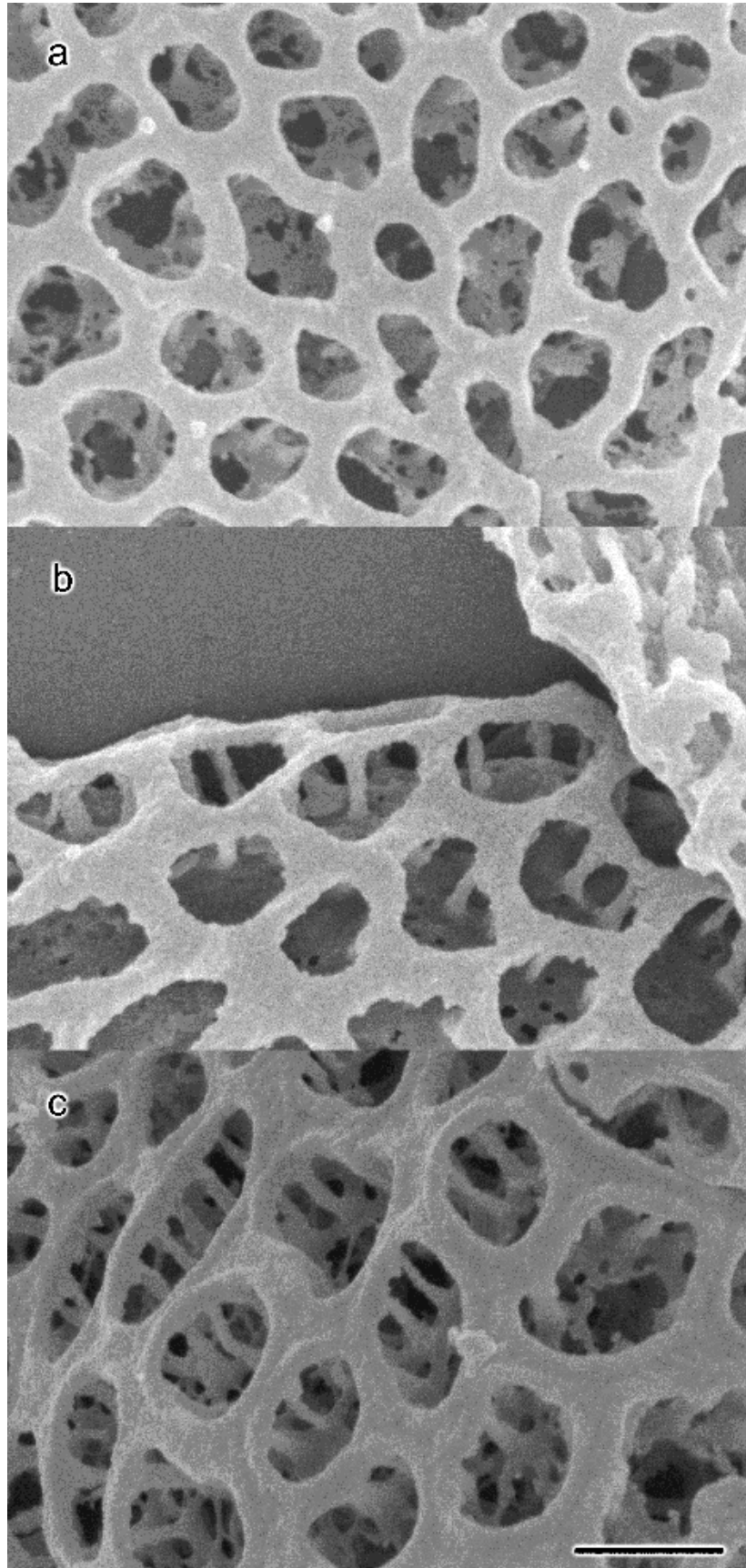
Chapter Four: *Arabidopsis* Pollen Developmental Series – Wild Type and Pollen Wall Mutants

Introduction:

To better understand the mechanism behind pollen and pollen wall development, a comparative analysis of the surface morphology of developing pollen grains in the model system *Arabidopsis thaliana* was conducted. Pollen wall mutants such as *defective in exine formation 1* (*dex1*), callose synthase 5 (*cals5*), and *thin exine 2* (*tex2*) are known to exhibit abnormal pollen walls as a result of aberrant development at one or more key events in the developmental process. For this reason, these particular mutants were chosen for this study.

Prior study of the *dex1* mutant line has determined the developing microspores exhibit a lack of normal plasma membrane undulation and abnormal sporopollenin deposition. This results in a discontinuous microspore wall, pollen degradation and ultimately, a male sterile flower. These alterations suggest that the *dex1* mutation disrupts normal primexine development, and subsequently, sporopollenin deposition and exine formation (Paxon-Sowders *et al*., 2001). Complementation experiments introducing the functional gene into the mutant line by means of *Agrobacterium* mediated transformation provided a successful recovery of the wild-type phenotype. This result confirmed that *DEX1* is the gene responsible for the male sterility phenotype observed. Northern blot analyses have revealed that *DEX1* transcripts are present in the wild-type bud, leaf, root and seedling tissue, with the greatest abundance localized to the bud tissue. Transcripts of *DEX1*, however, are lacking in the homozygous mutant. Despite the expression of *DEX1* in various wild-type tissues, no other blatant morphological defects were noted. Based

on this information, several roles of the protein have been proposed. Firstly, the DEX1 protein may function as a linker protein that resides within the plasma membrane of the microspore with the purpose of acting as an anchoring mechanism for initial sporopollenin deposition and proper exine formation. Alternatively, in place of anchoring to the sporopollenin directly, the DEX1 protein may instead adhere to the callose wall, enabling the ridges in the plasma membrane to form when the primexine matrix is deposited. If this proposal is accurate, it is likely that the protein would localize to the peaks of the undulating membrane. Lastly, the protein could be involved in processing of the primexine precursory material and closely associate with the rough endoplasmic reticulum. Though DEX1 shares no homologues in bacteria or animals, it is plausible that the protein functions similarly to α-integrins owing to the presence of a calcium binding domains, a cleavable signal sequence and a transmembrane domain (Paxon-Sowders *et al.*, 2001).

Callose is synthesized from glucose by a class of enzymes called callose synthases (Dong *et al.,* 2005). This compound has been found to play a variety of roles in developmental and reactive processes among plants. Callose is involved as a structural support of specialized cell walls. It aids in pathogen defense and the regulation of movement of molecules through the plasmodesmata from one cell to another (Chen and Kim 2009). Callose localizes to the phloem following injury and to the cell plate prior to cytokinesis and septum formation. Additionally, it has been proposed that callose plays a pivotal role in pollen development (Enns *et al.,* 2005). During pollen development in wild type (WT) *Arabidopsis*, callose deposition begins in late premeiosis. This causes a relative increase in thickness of the microsporocyte cell wall. As cytokinesis of the

coenocytic microsporocytes begins, the callose wall can be seen growing inward along the invaginations of the cell membrane. Following the completion of cytokinesis, the four microspores produced are fully encased in and separated by a wall of callose. In the *callose synthase* mutants (*cals5-3, cals5-4 and cals5-5*) however, the microsporocytes fail to synthesize callose for the external wall. This causes the developing microspores to exhibit severe deformation in which the proexine structures do not form. In lieu of a reticulate proexine, large spherical aggregates of sporopollenin can be observed on the microspore surface. It has been hypothesized that the callose wall may function as a trap or inhibitor of primexine, preventing the diffusion of the primexine into the anther locule and enabling exine to form (Nishikawa *et al.*, 2005). In addition, *cals5* mutants have been characterized by abnormally developed flowers with shrunken anthers that are partially or completely sterile. The siliques produced by a homozygous *cals5* mutant line were observed to be very short and contain few to no seeds. When emasculated *cals5* flowers are pollinated with WT pollen, normal fruit and viable seed is produced by the mutant. This information supports the hypothesis that the *cals5* mutation affects microsporogenesis only. The plasma membrane of developing microspores in *cals5* anthers are described as significantly different from the WT. While it appears flat in the WT, the plasma membrane of the mutant exhibits an irregular and wavy pattern. The intine was also observed to be unusual as it varied in thickness in the mutant pollen grains (Dong *et al.*, 2005).

A novel mutant termed *thin exine 2* (*tex2*) was recently described that also exhibits abnormal pollen wall formation. The *tex2* phenotype is characterized by fertile plants which produces mature pollen grains with an extremely thin exine layer. The

grains were described as 'glossy and sticky' and exhibit sensitivity to acetolysis. Additionally, the reticulate patterning observed in WT pollen grains is absent. The *tex2-4* allele exhibits normal pollen development until ring vacuolate stage of pollen development. At this point, microspores were observed exhibiting several abnormalities including cytoplasm shrinkage. Though the cause of the cytoplasm collapse remains unknown, two explanations have been proposed. The first suggests the collapse is a form of plasmolysis resulting from the constant changing of osmotic conditions due to a compromised exine wall. The second cites the shrinking as a symptom of programmed cell death. This particular phenomenon was also observed in other mutants with aberrant microsporogenesis. In *tex2*-4, the mature grains are completely disintegrated prior to anther dehiscence. Genetic analysis conducted indicated the *tex* gene is located at the bottom of chromosome five. Due to the novelty of the mutant line, it remains unclear as to which developmental process has been disrupted, resulting in the thin exine phenotype. It has been postulated that the T-DNA insertion may knock out a protein involved in primexine precursory material synthesis or transport (Dobritsa *et al.,* 2011). The value of the proposed technique was subsequently used to examine *Arabidopsis* pollen wall mutants. With this aim, we hope to elucidate how mutations at various developmental stages impact normal exine features and characterize novel features by SEM.

Materials and Methods:

Plant tissue used in this study was harvested from *Arabidopsis thaliana* ecotypes Columbia and Wassilewskija (WS). The *callose synthase 5-2* and *tex2-2* mutant lines in the Columbia background were obtained from ABCR (SALK_026354C and (SALK_001259 respectively). The *defective in exine formation 1* line in the WS

background has been continuously propagated from the same parental line that was deposited as CS382 by Christopher Makaroff. Seeds were planted directly to commercial potting mix (Sungro Metro Mix 360) and placed in a 20°C growth chamber under 16/8 hour light and dark cycle with 75% humidity conditions. All preliminary and troubleshooting experiments were conducted with *B. rapa* tissue owing to the ease with which the larger anthers could be excised. See Chapter One of this work for a more detailed description of the sample preparation.

Results:

Pollen development of the *dex1* line appears comparable to the wild type (Figure 14) and heterozygous tissue through meiosis and cytokinesis of the microsporocyte. Coenocytic microsporocytes of both WS wild type and *dex1* exhibit deep cleavage furrows and four lobes, presumed to be future microspores, of equivalent size and shape. The surface of the microsporocytes was relatively smooth. A number of holes ranging from three to four were observed in a linear orientation at the trough of the cleavage furrow (Figure 15a-b). The number and position of these pores are consistent with those observed in *Brassica rapa* cells at the same stage in development. These observations were consistent with those described by Paxon-Sowders *et al*. (1997). The microspore plasma membranes of both the heterozygous and mutant tissue remain level and nondescript (Figure 15c-d). Upon completion of cytokinesis, the primexine matrix is deposited at the surface of the plasma membrane. The heterozygous line begins to form undulations in the plasma membrane, creating an overall wavy appearance. The invaginations appear to form a recurring pattern (Figure 15e). The microspores of *dex1* showed no sign of surface invagination (Figure 15f). As development progressed in the

heterozygous line, small spheres of material, presumably sporopollenin, were observed collecting on the peaks formed by the invaginating membrane. These spheres coalesced to form contiguous structures reminiscent of tectum (Figure 15g). By contrast, despite the presence of spherical material appearing on the microspore, the surface remains uninvaginated. Islands of sporopollenin began to appear. The aggregates formed randomly about the surface of the microspore. Small pores, reminiscent of lacunae, were also observed in the islands of sporopollenin (Figure 15h). Deposition of material at the peaks of the ridges has increased in the heterozygous tissue such that the individual aggregates could no longer be discerned. In place of numerous spheres presides a single cohesive structure with a reticulate or latticed patterning residing primarily on the ridges of the membrane. In addition, the microspores exhibited regions or wedges with a flat appearance. A maximum of three per microspore was commonly observed. These features, presumed to developing apertures, were equidistant in position from one to the next (Figure 15i). By late tetrad stage, proexine structures such as protectum and pro-columella were observed. The overall latticed patterning was reminiscent of that present on a mature pollen grain, though highly compacted. Aperture regions are clearly defined. A brief qualitative analysis suggested a high proportion of the developing microspore is aperture. At an equivalent stage in development, the islands of sporopollenin continued to aggregate on the surface of the *dex1* microspores. Despite a seemingly random deposition of sporopollenin, the aperture regions remain clearly defined on the microspores (Figure 15j). Once released from the callose, the wild type microspores began to expand. The lacunae of the developing exine as well as the microspore itself were noticeably larger in diameter (Figure 15k). The released microspores of *dex1* exhibit large spheres of

sporopollenin that were variable in size. The pores presumed to be analogous to lacunae were no longer observed. Consistent with the data collected in previous studies, stages of development later than released microspore could not be found owing to the collapse of the released microspores (Figure 15l).

Callose synthase 5-2 like *dex1*, exhibits unusual pollen wall formation and demonstrates reduced male reproductive fertility. Distinct differences in relative thickness or consistency of the surrounding cell wall were observed as early as the microsporocyte stage (Figure 16a-b). Microspores of *cals5-2* at the early and middle tetrad stages exhibited the characteristic features that define each stage; either smooth or undulating surfaces respectively. Aperture regions could be found on the microspores of the middle stage (Figure 16c-i). As development progressed, small spherical objects, once again presumed to be sporopollenin, were observed accumulating at the peaks of the ridges in both mutant and wild type (Figure 16g-h). Evidence of aberrant wall development began at the late tetrad stage. The overall construction of the exine was more muddled than that of wild type. The developing wall exhibited a porous construction in discrete areas. The aperture regions observed at early stages were no longer discerned (Figure 16j). The released microspore stage exhibited spheres of sporopollenin covering the microspore surface. These aggregates were irregular in organization and highly variable in size. The aperture regions remained obscured (Figure 16l).

The final mutant involved in this study, *tex2-2*, demonstrated a development consistent with the wild type up through middle tetrad stage. Superficial examination of the coenocytic microsporocytes of *tex2-2* revealed no abnormalities compared with the

wild type. Cytokinesis appeared typical. The four lobes of the future microspores were relatively equivalent in size in both wild type and mutant. The microspores of *tex2-2* at the early and middle tetrad stages exhibited the typical features associated with each stage in development. The early tetrads of *tex2*-2 demonstrated a featureless surface (Figure 17a-b). At the subsequent stage, the mutant microspores exhibited an undulating plasma membrane. Smooth regions presumed to be future sites of apertures could be observed. Commonly, three aperture regions were observed on a single microspore, and appeared equidistant from one to the next (Figure 17c-d). At this point in development, however, the microspores of *tex2-2* begin to exhibit atypical features. In wild type, small spheres of material can be observed collecting on the ridges of the undulating membrane. While *tex2-2* does produce these spheroidal objects, the deposition of this material is not strictly localized to the peaks of the ridges (Figure 17d-e). As deposition continues through development, the spheroidal objects become more pronounced as well as numerous. The aggregates ultimately covered the aperture regions in the later stages of tetrad development (Figure 17f-h). It was not uncommon to observe the material to fail to adhere and fall away from the microspores.

Discussion:

In this chapter, the protocol devised using mechanical pressure and enzymatic digestion to expose developing microspores was employed to elucidate the development of the exine of three pollen wall mutants. The pollen wall mutants chosen for this study were aberrant in one or more steps of development. The mutant *defective in exine formation 1* (*dex1*) microspores exhibit abnormal sporopollenin deposition and a lack of normal plasma membrane undulation (Paxon-Sowders *et al*., 2001). Plants containing the

callose synthase 5 (*cals5*) mutant gene demonstrate a reduction in callose deposition at the periphery of the microsporocytes (Dong *et al*. 2005) The *thin exine 2* (*tex2*) mutant lines, though novel and with a phenotype that is mechanistically enigmatic, have demonstrated aberrant wall formation in the form of an extremely thin exine and lack of the characteristic lattice patterning (Dobritsa *et al.,* 2011).

The analyses by SEM of the pollen wall mutants appear to be consistent with the observations noted in previous studies. Abnormalities in development became evident in the various mutants at the tetrad stage. Microspores at the middle tetrad stage of *dex1* lacked membrane undulations. The sporopollenin deposited at this stage appeared random atop the surface. Microspores of *cals5-2* and *tex2-2* progressed further in development, through middle tetrad stage, before the emergence of aberrant features. By late tetrad stage, abnormal deposition of sporopollenin could be observed in all of the mutant lines. It is interesting to note that while the aggregates that formed in the *dex1* and *cals5* mutant lines had a tendency to coalesce into spheres of variable size with sustained deposition, the sporopollenin deposits present on the *tex2-2* mutant remained small and relatively uniform in size.

Microspores of *cals5* at an equivalent stage of development exhibited characteristic surface undulations similar to that of the wild type. As deposition progressed, large spheres of sporopollenin of variable size were observed on both mutants. Microspores of the *dex1* mutant ultimately collapsed following the dissolution of the callose wall. A closer examination of the sporopollenin aggregates revealed the appearance of a superficial polygonal patterning exclusively on these structures. The patterning was comparable to that of the patterning of a mature pollen grain. Whether this

distinct patterning is a result of sporopollenin subunits assembling or an artifact from sample preparation is as yet unknown. Due to the frequency with which this patterning was observed in the two different mutant lines, however, it is unlikely to be an artifact induced by preparation of the samples.

Interestingly, the presence of apertures at various stages in development could be observed amongst the mutant lines. Despite abnormal callose deposition, *cals5* presented normal apertures at the early stages of tetrad development (Figure 18a). Both the distribution and relative thickness appeared consistent with the wild type. Early tetrad microspores of *tex2-2* also exhibited apertures consistent with wild type (Figure 18b). While the lack of membrane undulations made determining aperture formation difficult in *dex1*, later tetrad stages still exhibited regions of no or reduced sporopollenin deposition (Figure 18c). Despite the differences in breakdown of the sporopollenin deposition machinery in the various mutants, the designation and formation of the aperture regions remained, at least in early development. This appears to indicate that aperture formation is highly controlled and involves a protein or network separate from but in tandem with that which is involved in sporopollenin deposition. This postulation is not without merit as a novel protein named INAPERTURATE POLLEN1 (*INP1*) was recently examined for its role in aperture formation in *Arabidopsis*. INP1 is produced by the microsporocyte prior to meiosis and remains present in the microspore progeny following cytokinesis. This protein, when tagged with YFP, was found to localize to and position along regions of future apertures (Dobritsa and Coerper 2012).

Figure 14: Early pollen developmental series of Wassilewskija ecotype of *Arabidopsis thaliana.* (a) Coenocytic microsporocyte free of callose wall. The four lobes of the future microspores were present. (b) Early or 'young' tetrad stage microspore with smooth surface and distinct angularity. (c) Middle tetrad microspore with periodic and regular indentation of the plasma membrane. (d-e) Middle tetrad microspore with small aggregates on the ridges. (e) Late tetrad microspore with a unified tectum. Latticed patterning was recognizable. The apertures were readily apparent. Size bars (a) measure 5 µm; (b-f) measure 2 µm.
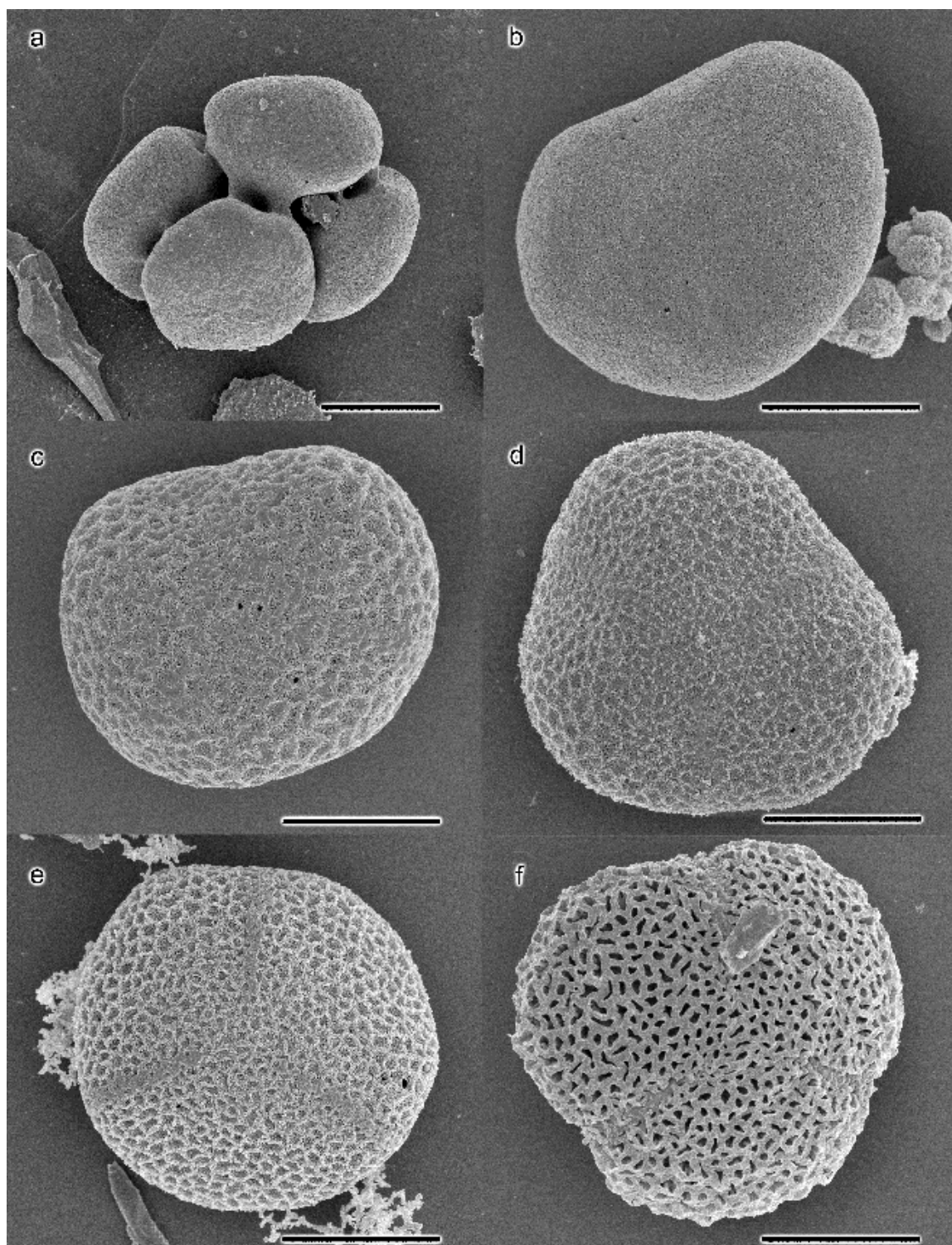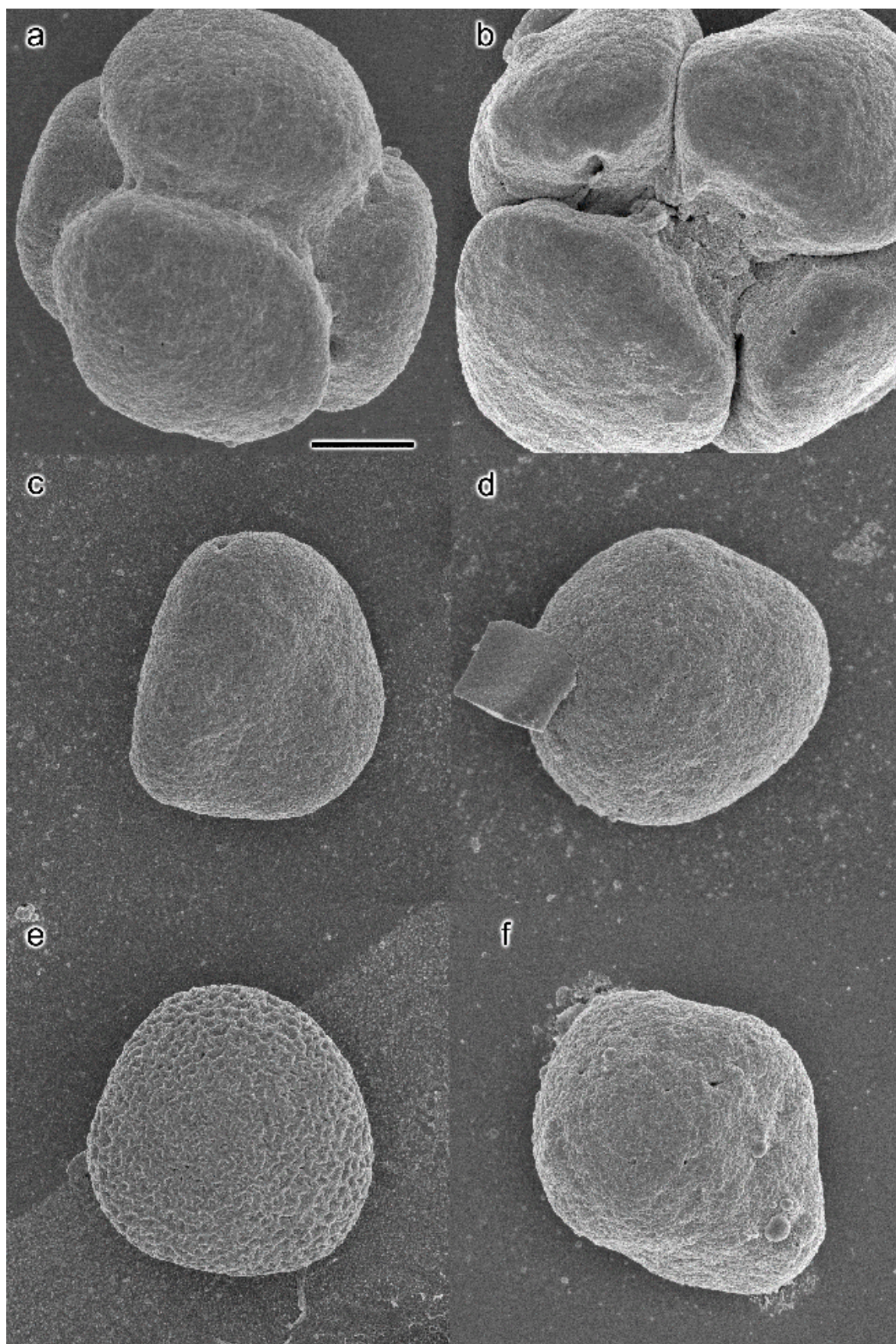
Figure 15: Early pollen developmental series of *dex1* heterozygous and homozygous lines in *Arabidopsis thaliana*. Micrographs a, c, e, g, i and k represent microspores from the *dex1* heterozygous line. Micrographs b, d, f, h, j, and l represent developing microspores from the *dex1* homozygous line. (a-b) Coenocytic microsporocytes in the process of cytokinesis. (c-d) Early tetrad microspores. (e-f) Middle tetrad microspores with periodic and regular indentation of the plasma membrane in the heterozygous line. (g-h) Middle tetrad microspores during the initiation of sporopollenin deposition. (i-j) Late tetrad microspores. (K-l) Released microspores. Size bars measure 2 μm for all micrographs.

Figure 16: Early pollen developmental series of *cals5-2* and Columbia ecotype in *Arabidopsis thaliana.* Micrographs a ,c , e, g, i and k represent microspores from the Columbia ecotype. Micrographs b, d, f, h, j, and l represent developing microspores from the *cals5-2* line. (a-b) Microsporocytes prior to or during cytokinesis. Distinct differences in relative thickness of the surrounding cell wall were observed. Tissue was not subjected to digestion. All subsequent tissue was digested with cytohelicase. (c-d) Early tetrad microspores. (e-f) Middle tetrad microspores. (g-h) Middle tetrad microspores during the initiation of sporopollenin deposition. (i-j) Late tetrad microspores. (K-l) Released microspores. Size bars measure 2 μm for all micrographs.
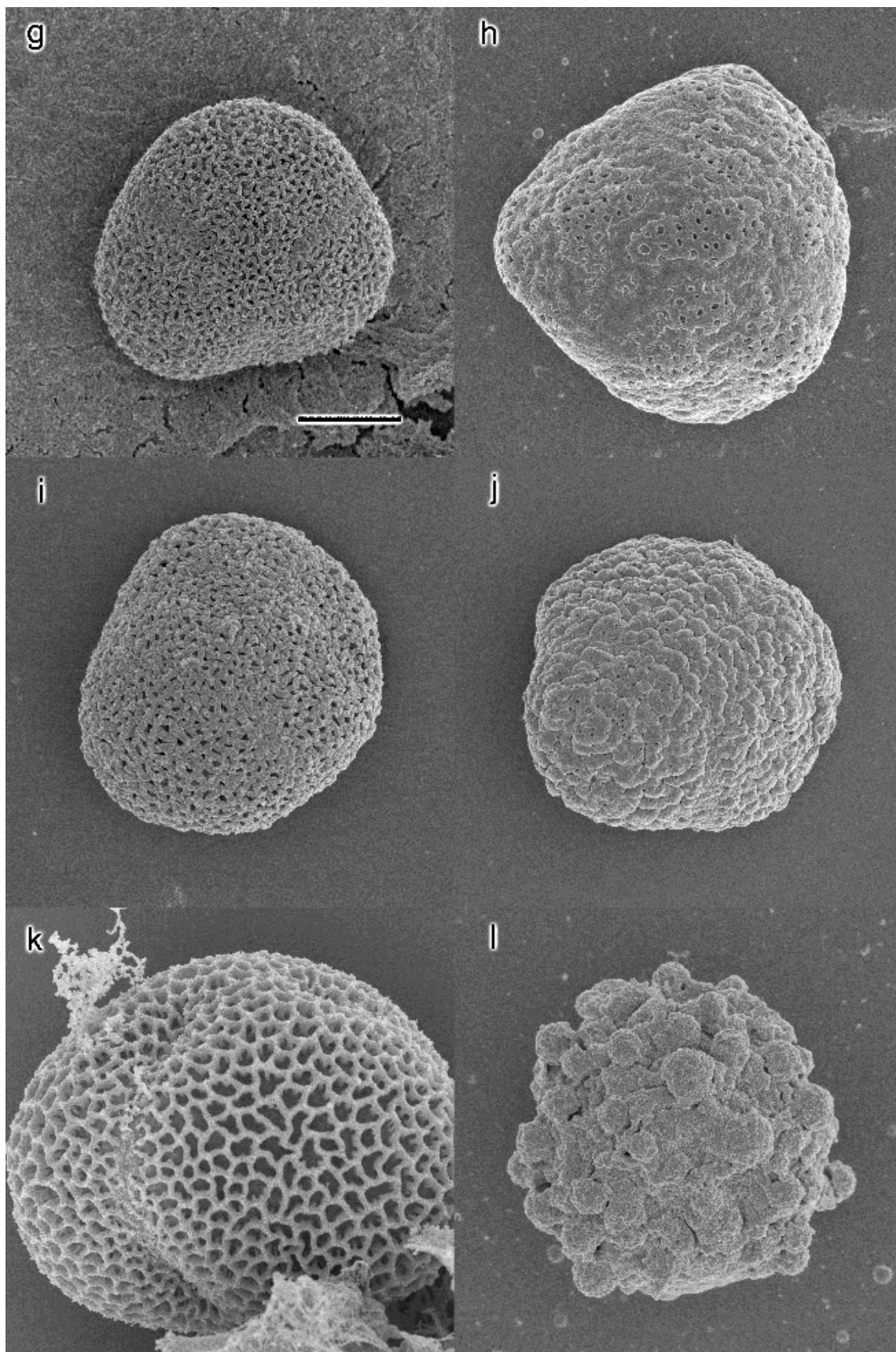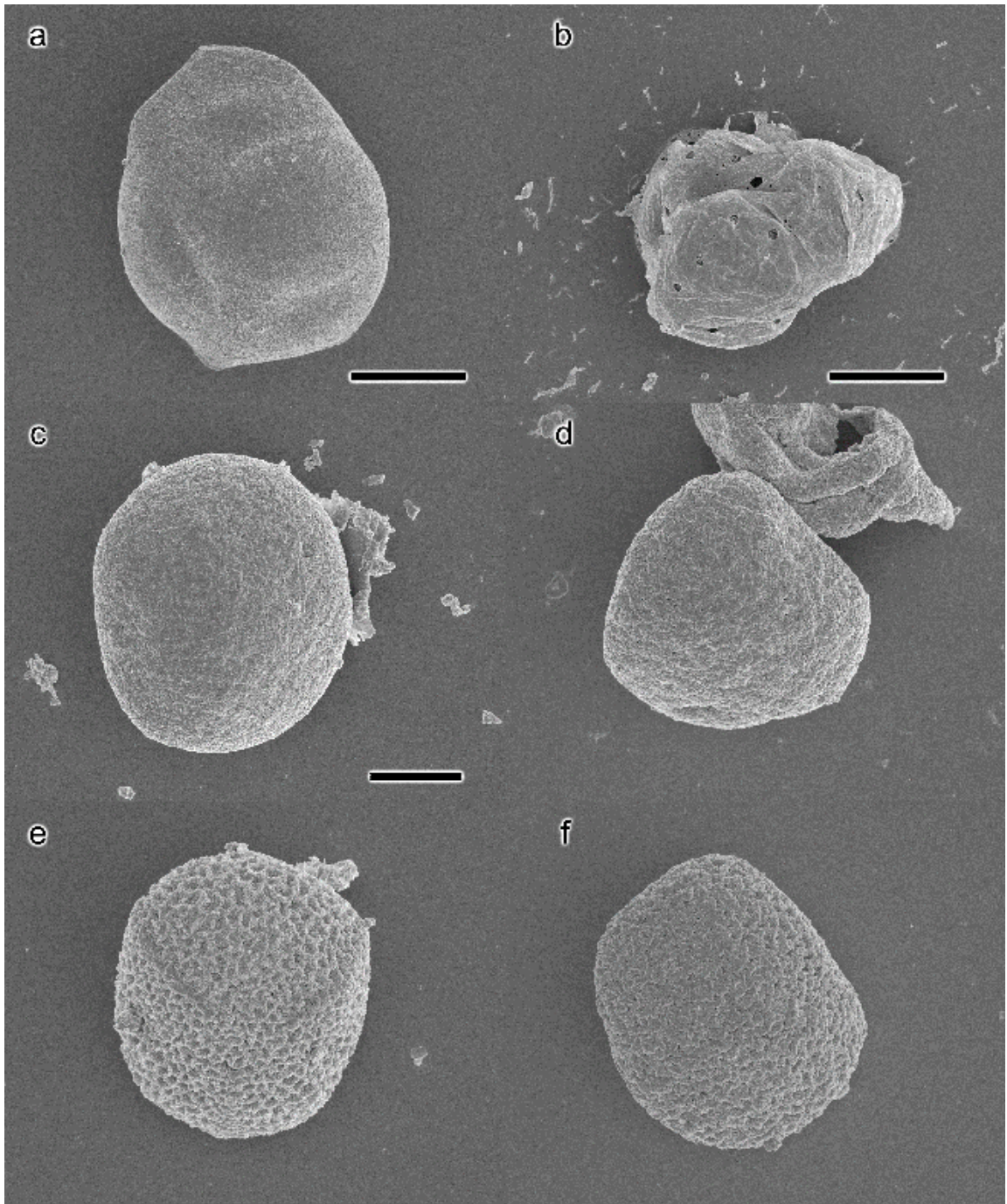
Figure 17: Early pollen developmental series of *tex2-2* in *Arabidopsis thaliana.* (a) Coenocytic microsporocyte during the process of cytokinesis. (b) Early tetrad microspore. (c-d) Middle tetrad microspores with periodic and regular indentation of the plasma membrane in the heterozygous line. (e) Middle tetrad microspore during the initiation of sporopollenin deposition. (f-g) Late tetrad microspores. (h) Released microspore. Size bar measures 2 µm for all micrographs.

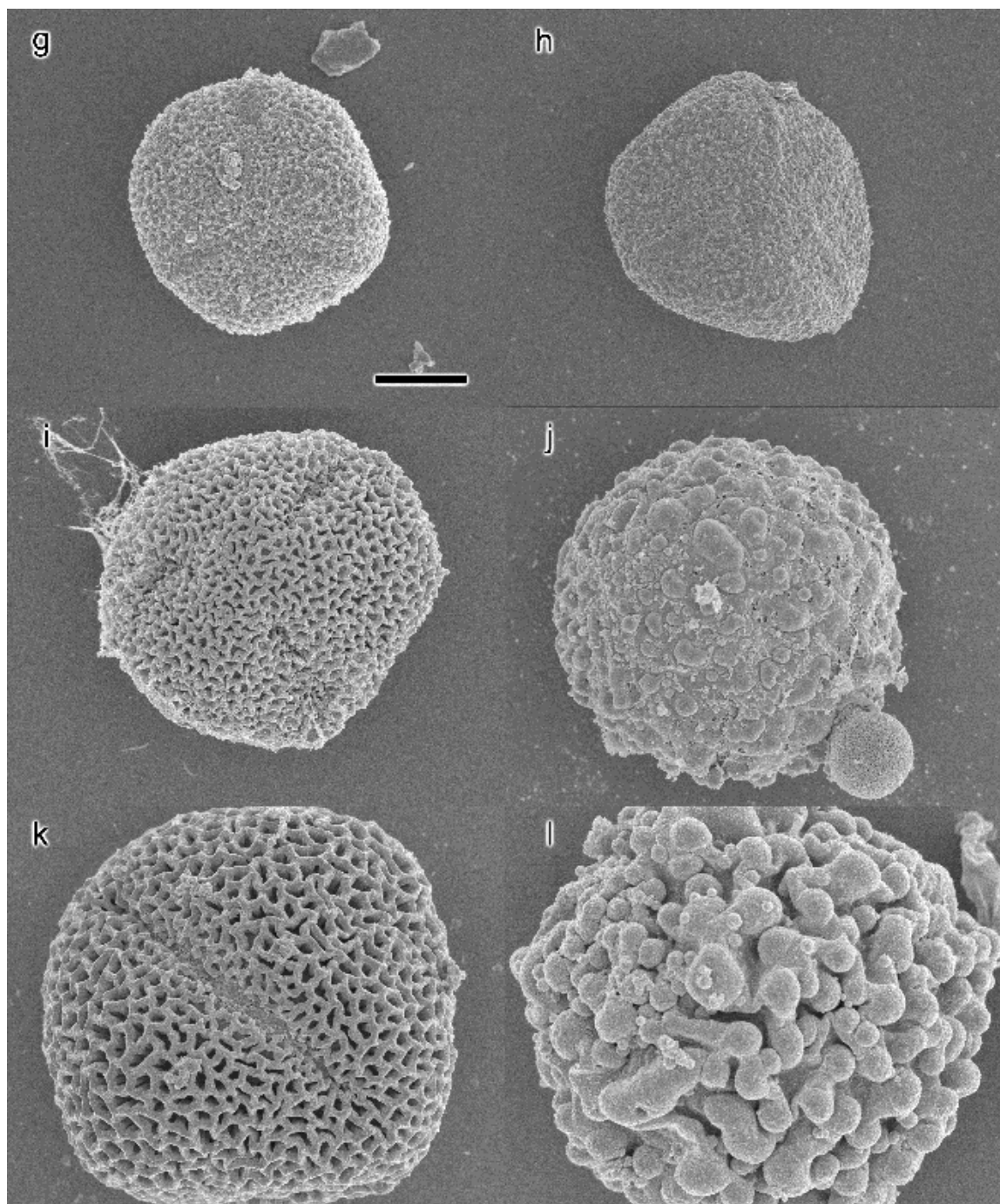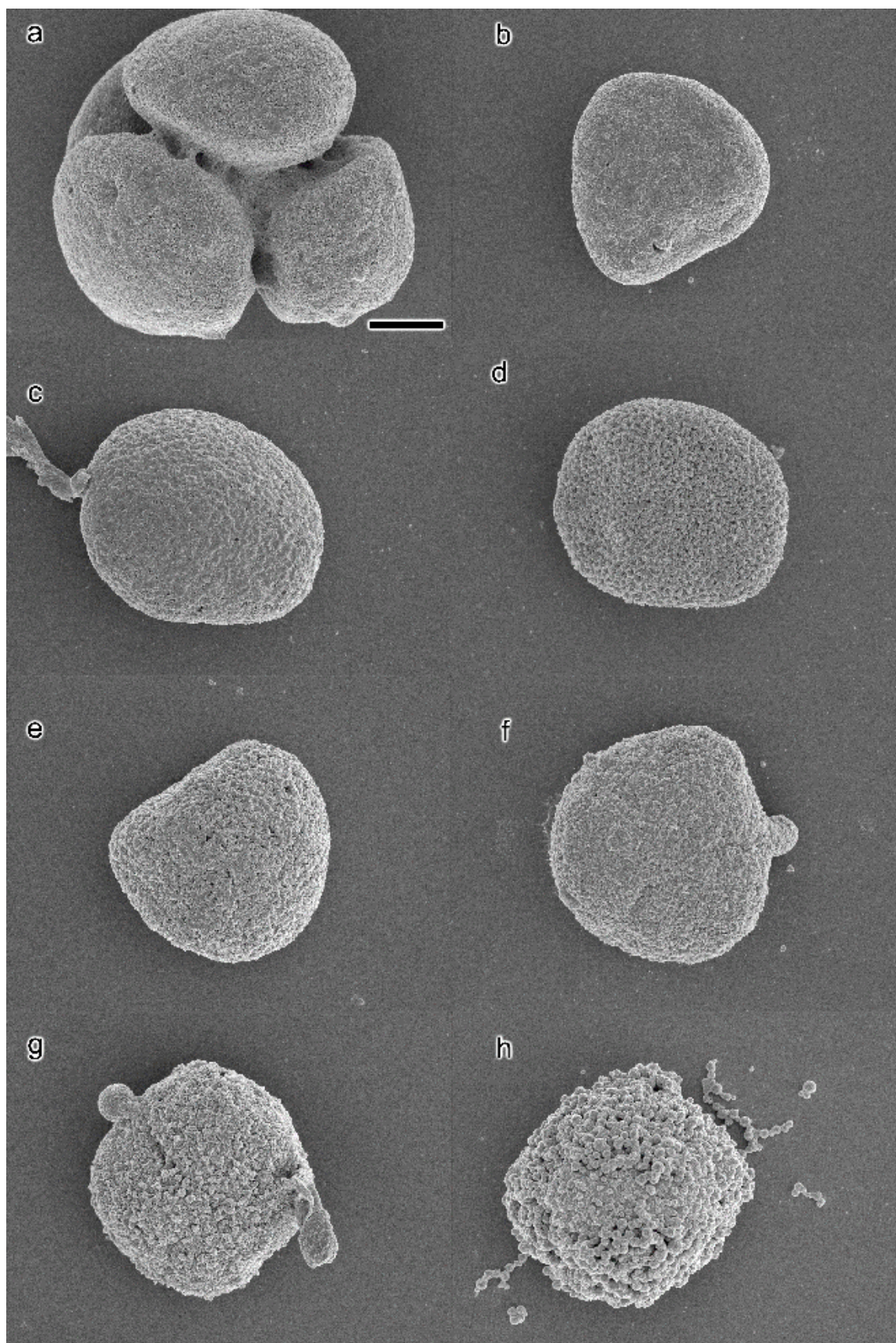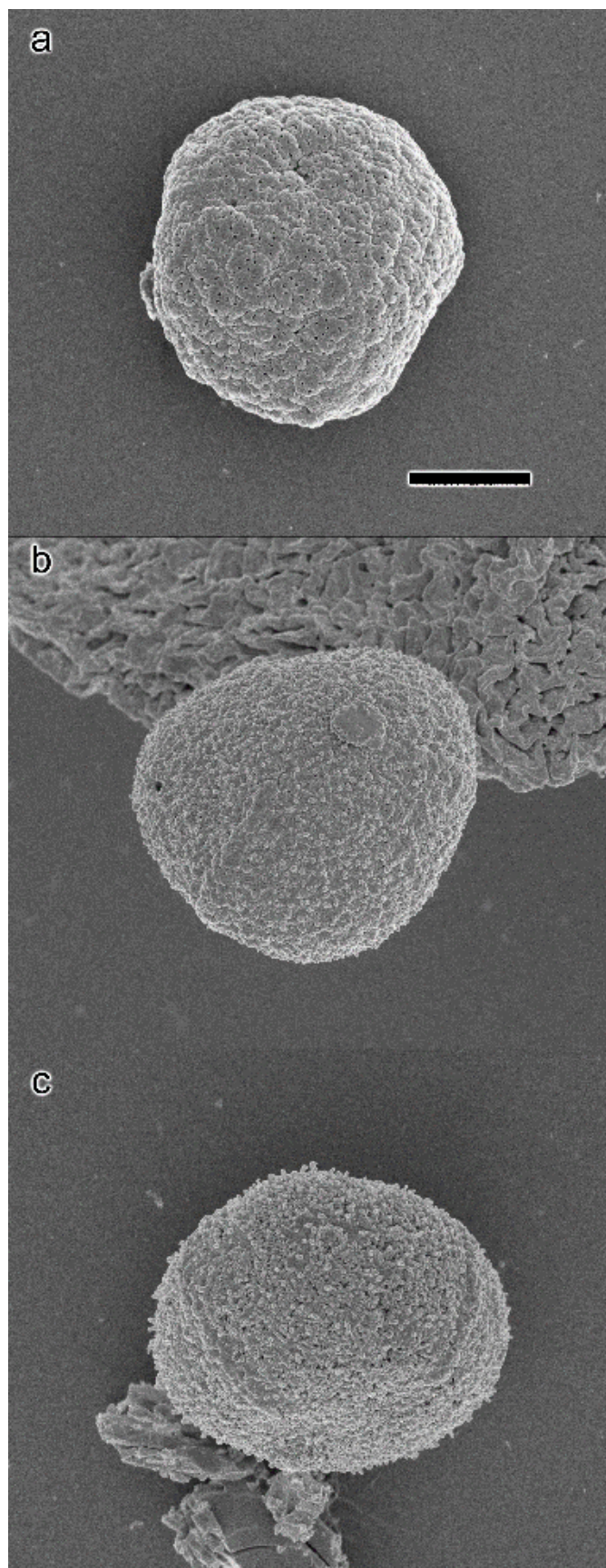**Figure 18:** Early exine of mutant microspores depicting aperture regions. (a) Late tetrad microspore of *dex1* homozygous line. (b) Middle tetrad microspore of *cals5*-2. (c). Middle tetrad microspore of *tex2-2*. Size bar measures 2 μm for all micrographs.

Chapter 5: Immunolabeling and Localization of DEX1

Introduction:

Detailed molecular studies conducted previously on the *dex1* mutant line have found several similarities to various adhesion proteins. Among them, the greatest commonalities were found in the class of proteins called α-integrins and cadherins. Several features common to both classes of proteins include a transmembrane domain, numerous glycosylation sites as well as a cleavable amino acid signal sequence at the carboxyl-terminal end of the polypeptide and an affinity for binding to calcium. It has been postulated that DEX1 shares many of these features. Based on the molecular analyses of the transcript and polypeptide sequences, it was predicted that DEX1 functions similarly to a type 1a membrane protein with a proclivity for membrane localization. DEX1 also exhibits 12 different glycolsylation sites, and contains multiple domains capable of binding calcium. Based on the molecular and ultrastructural studies, multiple hypotheses for the function of the DEX1 have been proposed. First, the protein will localize to the valleys of the undulating membrane and interact with cytoskeletal elements to aid in the repositioning of the plasma membrane away from the callose wall. Conversely, the protein may localize to the crests of the undulating membrane. It has been hypothesized that in this position, the protein functions as an anchoring mechanism by binding directly to the callose wall. In either case, a portion of the protein is present on the surface to act as a nucleation point for sporopollenin deposition (Kostic 2004).

To further elucidate the role of DEX1 in pollen wall development, immunocytochemistry was conducted on developing microsporocytes and tetrad stage microspores to determine the relative localization and distribution of the plant protein

DEX1. Immunocytochemistry is a molecular recognition technique that assesses the presence of a particular target or antigen. The process involves localizing the desired antigen by incubating tissue with antibodies specifically directed to bind to a region or regions of the antigen. The antibodies themselves are conjugated to a visual tag, such as a fluorochrome or metallic nanoparticle. To observe the relative location of the desired protein within a cell or tissue, one must only look for the visual tag. To localize the protein, the tissue antigen is exposed to a primary antibody, which is usually generated in a species different from that which produced the antigen of interest; commonly referred to as the second species. After binding is achieved, the tissue is incubated with a secondary antibody against the primary antibody. The secondary antibody is produced in a third species to react against antibodies created by the second species and is conjugated to a visual tag. This method is often favored as secondary antibodies are relatively easy to produce and multiple secondary antibody containing tags are capable of binding to the target. This amplifies the signal to produce a strong localization of the target antigen (Bozzola and Russel 1999).

The production of antibodies, though conceptually simple, often produces unanticipated outcomes. Individual animals used in the production of the antibodies can respond differently to the same antigen. This results in antibodies with different binding affinities for the same antigen. The species in which the antibody was produced can also influence the effectiveness of the final product. In addition, unlike the conventional immunocytochemistry adapted to mammalian systems, plant tissue provides unique barriers that must be overcome. The cell wall, for example, becomes an excellent barrier to the infiltration of objects like antibodies into the cell body itself (Vaughn 2013).

Preliminary data indicated that despite the lack of transcript present in the homozygous tissue (Paxson-Sowders *et al.* 1997), the signal from the gold conjugate labeling the DEX1 protein was observed on both the homozygous and heterozygous tissue. This labeling localized to the periphery of the microspores and the surrounding callose walls or starch granules (Owen personal communication). The lack of specificity of the primary antibody was proposed to result from the primary antibody recognizing and binding to similar epitope regions of complex polysaccharides and glycoproteins. In fact, Western blots using this antibody against protein isolated from WT and *dex1* plants performed by April Wang demonstrated the extent of extraneous labeling by the primary antibody.

One way to overcome this barrier is through the complete removal of the cell wall. The primary cell wall is a complex and heterogeneous matrix of polysaccharides. One element of the cell wall consists of a group of polysaccharides known as pectins. Pectin molecules are linked together into extensive networks with both covalent and ionic bonding. These linkages are facilitated by the presence of either boron or calcium. Homogalacturonan, also referred to as polygalacturonic acid, is one such constituent of pectin network that utilizes calcium to crosslink the carboxyl groups present on the molecule. The cross-linking effectively forms a stiff gel that stabilizes and strengthens the cell wall (Cosgrove 2005). Preliminary data suggests floral tissue incubated in PFA (Wick 1993) for an extended period of time enables the separation of the microsporocytes and tetrad microspores from their surrounding wall when gently squashed. It has been proposed that the prolonged exposure to a calcium chelator, as EGTA is a primary

component of Wick's PFA, is loosening the pectin bonds and enabling the clean removal of the cell wall (Owen personal communication).

It is the intent of this study to further elucidate the function of DEX1 through an accurate assessment of the localization of the DEX1 protein. Due to the absence of DEX1 specific binding of the primary antibody, this study will evaluate various techniques involving a removable embedding media as well as incubation with a calcium chelator to remove the callose and vegetative cell walls in order to reduce nonspecific labeling.

Materials and Methods:

Tissue was collected from plants of the *dex1* mutant line #8.090206074902020101. Seeds were first surface sterilized as follows. Approximately 100 to 200 seeds were placed in a 15 mL vial containing 1 mL of a Clorox solution (6% sodium hypochlorite and 1-2 drops Tween-20). The seeds were incubated in the Clorox solution for 8 minutes. Care was taken to not leave the seeds in the solution longer than 8 minutes for risk of phytotoxicity. A glass Pasteur pipet was used to swirl and mix the contents of the vial in order to 'declump' and remove any seeds that adhered to the wall of the vial. After the incubation time elapsed, the vial was filled with distilled water. The contents of the vial were swirled to ensure thorough mixing followed by allowing the seeds to settle to the bottom. All but approximately 1mL of the fluid was siphoned off and replaced with fresh distilled water. The seeds were rinsed in this fashion a total of three times. Upon completion of the final rinse, the fluid was once again siphoned off using a glass pipet, leaving approximately 1mL covering the seeds. 2-4mL of ethanol was added to the vial. The contents was mixed, siphoned into a pipet and rapidly transferred onto a 9 cm Whatman #1 filter paper draped over the mouth of an empty 50 mL beaker.

The seeds were then allowed to dry in a sterile transfer hood for 15-20 minutes before being stored in a sterile glass Petri dish.

In a sterile transfer hood, the sterilized seeds were transferred to MS media (MP Biomedical 0926232) growth plates inoculated with the selective agent Kanamycin. Kanamycin resistance was used to monitor the segregation of seedlings containing T-DNA insertion (Feldman and Marks 1987). Plants were grown on the plates under a 16/8 hour light cycle and room temperature conditions. Once the hypocotyls reach a height of approximately 1 cm, the juvenile plants were transplanted to moist soil, taking care not to damage the radical. Pots were placed in a covered container before being transferred to a growth chamber set to 20°C and 16/8 light cycle. Plants remained covered for a minimum of 4 days, after which the cover was removed.

Inflorescences were harvested prior to bolting and immediately fixed in a solution of 2% gluteraldehyde in 0.1M HEPES buffer and 0.05% Triton-X (Makaroff and Owen 1995). Plant material was allowed to fix for a duration of approximately 14 hours. Inflorescences were subsequently rinsed two times with 0.1 M HEPES for 15 minutes each.

The following protocol is outlines in Figure 19. Following fixation, tissue was dehydrated in a graded ethanol series. HEPES buffer was replaced with 10% ethanol. Tissue was incubated in the ethanol for one hour. The plant material was then transferred to successively higher concentrations of ethanol which increased in increments of 10%. Incubation time within each step remained one hour. The dehydration of the plant tissue culminated with rinsing the tissue in 100% absolute ethanol several times for an hour each rinse. Following dehydration, the absolute ethanol was exchanged with n-butyl

alcohol over several changes. This transition step is required as diethylene glycol distearate (EMS 14010) is not soluble in ethanol. The incubation times were substantially increased from the protocol established by Capco *et al.* (1984) owing to the presence of the relatively impermeable cell wall. The tissue was transferred to a 1:1 mixture of n-butyl alcohol to absolute ethanol and allowed to incubate for a minimum of one hour before a second change was made. A second incubation in a 2:1 mixture of n-butyl alcohol to absolute ethanol was conducted in a similar fashion prior to transferring to 100% n-butyl alcohol. Several changes of n-butyl alcohol were conducted over several hours. Diethylene glycol distearate (DGD) was melted in a glass beaker at 65°C. Once molten, the DGD was filtered through grade 1 9 cm Whatman #1 filter paper (Cat No. 1001 090). The tissue was transferred to a 1:1 and 2:1 mixture of filtered DGD to n-tbutyl alcohol in a manner consistent with the methodology described above. Following the final incubation in the DGD/n-butyl alcohol mixture, the inflorescences were infiltrated with 100% pure DGD over several days. The tissue was kept at 65°C to ensure the DGD remained molten (Taleporos 1974; Capco *et al.* 1984). Prior to embedding, the silicon embedding mold (Ted Pella; 10505) was heated on a slide warmer to approximately 70°C. The infiltrated buds were excised individually and oriented in the warmed mold with the top of the bud facing the narrow end of the well of the mold. The mold was allowed to cool overnight at room temperature.

Blocks of DGD were removed with great care from the embedding mold to prevent fracturing of the block. In addition, gloves were worn during the removal process to prevent oils and contaminants from interacting with and softening the block. Contrary to conventional ultramicrotomy, the blocks were not block-faced prior to sectioning.

Traditional block-facing produces minute fractures that permeated the block. These fractures caused the block to fragment upon sectioning. For this reason, bud orientation and placement is of the utmost importance during the embedding process.

Blocks were sectioned with a RMS MT-7 Ultramicrotome on a dry glass knife. The knife angle utilized during sectioning was set to 10°. Sections 3-4µm in thickness were cut from the block and transferred to water on a poly-l-lysine coated coverslip and left to dry down onto the coverslip at room temperature overnight. Sections were placed onto a drop of water to allow for decompression of the section.

After drying to the coverslip, the sectioned tissue was stored in 100% n-butyl alcohol for a minimum of 16 hours with several changes of fresh n-butyl alcohol during that time in order to remove the wax. The coverslips were returned to 100% ethanol through a graded n-butyl alcohol/ethanol series in a concentration of 2:1 and 1:1 respectively. The sample was ultimately rinsed twice with absolute ethanol for one hour per rinse (Capco *et al.* 1984; Nickerson *et al.* 1990). The ethanol was later replaced with liquid carbon dioxide and the tissue critical point dried using a Balzers Union CPD 020 model drier. The coverslips were mounted onto specimen stubs before receiving a layer of colloidal graphite at the periphery of the coverslip and coated with 4 nanometers of iridium using an Emitech K575X sputter coater. The prepared samples were observed using the Hitachi S-4800 scanning electron microscope. Any image editing for manuscript figure construction was conducted using Photoshop v.5.5 for windows.

Immunolabeling on embedment-free sections was conducted prior to critical point drying. Tissue was dried onto coverslips coated with poly-l-lysine and returned to 100% ethanol as previously described. The coverslips were then rehydrated in increments of

20%. Incubation in each increment was a minimum of one hour. The following immunolabeling protocol was adopted and modified from Swatzell *et al.* (1999). Tissue was blocked with 3% bovine serum albumin (BSA) in 0.01 M Tris, 0.15 M NaCl buffer (pH 7.4) for 1 h according to the protocol by Smallwood *et al.* (1995). The coverslips were then rinsed with tris-buffered saline (TBS) 10 times, removing excess buffer between rinses. A dilution of 1:60 of the rabbit anti-dex1 antibody was created in buffer. The sample was incubated in the primary antibody for a minimum of one hour. Incubation overnight at 4°C is also recommended to increase likelihood of antibody binding to desired epitope. Following this incubation, the coverslips were rinsed 10 times with buffer. The sample was then incubated with Protein A conjugated to 20nm colloidal gold (Sigma: P6855) followed by a third series of rinses with buffer. In order to crosslink the gold conjugate with the primary antibody and protein of interest, the sample was treated with a fixative. Following the final rinse in TBS, the coverslips were rinsed twice with distilled water. The sample was transitioned to PBS buffer with two rinses for thirty minutes per rinse. 1% gluteraldehyde in phosphate-buffered saline (PBS) was then applied to the coverslips and allowed to incubate for one hour. The coverslips were thoroughly rinsed with distilled water, dehydrated in a graded ethanol series and critical point dried in a manner consistent with the protocol previously described. The coverslips were mounted onto 25 mm specimen stubs before receiving a layer of colloidal graphite at the periphery of the coverslip and coated with 2 nanometers of iridium using the Emitech K575X sputter coater. The addition of the colloidal carbon paint and iridium is utilized to enhance conductivity of a naturally nonconductive sample. The samples were observed using the Hitachi S-4800 scanning electron microscope and photodiode

backscattered electron (BSE) detector from Hitachi. Any image editing for manuscript figure construction was conducted using Photoshop v.5.5 for windows.

Tissue treated with Ethylene glycol-bis(2-aminoethylether)-N,N,N′,N′-tetraacetic acid (EGTA) prior to immunolabeling was handled as follows. Anthers were fixed and staged according to the protocol previously described. The remaining anthers were excised and incubated in 100mM EGTA for a minimum of 24 hours in a cavity slide. Following incubation, the tissue was rinsed three times in distilled water for ten minutes per rinse. As the size of the anthers borders on the miniscule, great care must be taken to insure the anthers remain within the well during the rinsing process. Pressing a glass pipet tip firmly against the base of the well during the siphoning process helps to reduce the probability of losing the specimen. The anthers were collected using a dissecting needle and placed on a coverslip coated with poly-l-lysine. The tissue was subsequently squashed and prepared for viewing by SEM in a manner similar to that previously described in chapter one.

Results:

Embedment free sections: DGD

To detect the gold conjugate by SEM, the sections were viewed with the Hitachi photodiode backscattered electron detector. As expected, the signal from the gold conjugate labeling the DEX1 protein was observed on both the homozygous and heterozygous tissue. Labeling localized to the periphery of the tetrad microspores as well as heavily on the callose wall as a result of an impure primary antibody. The lack of specificity of the primary antibody was consistent with the findings by Kostic (2004).

However, discrete groupings of gold conjugate were observed at the periphery of the heterozygous tissue that was not observed in the homozygous tissue (Figure 15).

To overcome the problem with the primary antibody, the tissue was placed in a removable embedding media to allow the enzymatic digestion of the callose wall. Though cumbersome, the infiltration and sectioning of the tissue proved successful in DGD. Despite prolonged incubation in both solvent and enzyme, however, the enzymatic digestion of the callose wall could not be obtained (Figure 16). Enzymatic digestion of fresh anther tissue at the microsporocyte and tetrad stages proved insufficient and success was variable between treatments. Microspores early in development, prior to callose synthesis, often retained the primary cell wall (data not shown).

Tissue incubated with 100 mM EGTA demonstrated a clean separation of the cell wall and protoplast by light microscopy. When viewed under greater magnification by SEM, the surface of the microsporocytes and tetrad microspores exhibited severe deformation. Numerous pores were observed, often exposing the intracellular contents.

Discussion:

Preliminary data involving immunolabeling of *dex1* found labeling at the periphery of developing microspores. Discrete groups of localized label were observed only in the heterozygous tissue. This phenomenon is consistent with data produced in previous studies (Paxon-Sowders *et al.* 1997; Kostic 2004). Labeling experiments of homozygous tissue also demonstrated heavy labeling of the callose and vegetative cell walls. This non-specific labeling, as the *dex1* mutant has no protein transcript, seems to suggest that DEX1 shares structural similarities with other complex carbohydrates and other cell wall constituents. As previously indicated, it is understood that DEX1 exhibits

several glycolsylation sites. While it is assumed the primary antibody can bind to the protein, due to the presence of discrete groupings of gold label observed on the heterozygous tissue, it is possible that the additional aberrant labeling may result from an epitope similarity between the polysaccharides present at the glycolsylation sites of DEX1 and the constituents of the cell wall.

To reduce the excess labeling, numerous methods were utilized in an attempt to free the microsporocyte from the encapsulating cell wall and other extraneous elements that the primary antibody has binding affinity for. Infiltration of the anther tissue with the removable embedding media DGD proved unsuccessful as the callose wall could not be digested away following the extraction of the embedding wax. Incubating the tissue with a calcium chelator like EGTA proved effective in separating the microsporocyte from the cell wall. The resulting sample, however, demonstrated severe deformation and was deemed unsuitable to progress with immunolabeling.

Despite these efforts, an effective means of removing the callose and primary cell wall while preserving the underlying surface remains elusive. The next appropriate step would be to attempt primary antibody purification or obtain monoclonal antibodies to DEX1.

Figure 19: General schematic of tissue preparation with DGD. Diagram depicting the general steps involved in preparation and sectioning tissue infiltrated with DGD prior to immunolabeling or SEM observation.

Sample Preparation in DGD → Tissue fixed in 2% gluteraldehyde → Rinse twice in 0.1 M HEPES

Incubate in 100% n-butyl alcohol ← Incubate in 1:1 & 2:1 mixture of n-butyl alcohol to absolute ethanol ← Dehydration in EtOH - 10% increments

Incubate in 1:1 & 2:1 mixture of filtered DGD to n-butyl alcohol → Infiltrate tissue with 100% molten DGD over several days → Embed in silicon molds and allowed to harded overnight

Incubate in 100% n-butyl alcohol for minimum of 16 hours ← Transfer to water drop on coverslip and allowed to dry down overnight ← Section tissue with glass knife to make 3 -4 μm sections

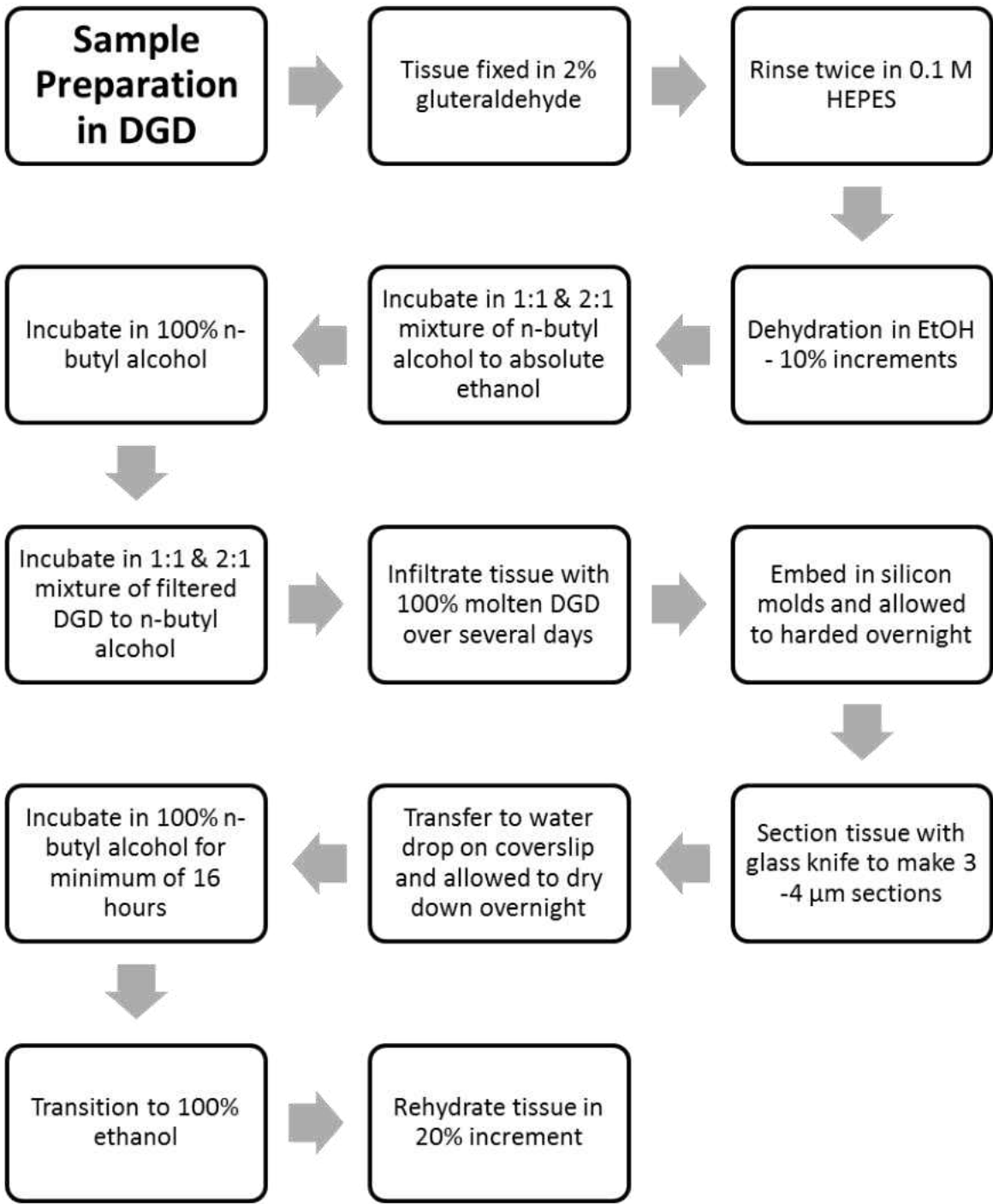Transition to 100% ethanol → Rehydrate tissue in 20% increment

Figure 20: Preliminary immunolabeling of *dex1* sectioned tissue with gold conjugate. (a-b) Backscattered electron micrographs of sectioned heterozygous tissue labeled with secondary 18 nm gold. (c-d) Backscatter micrographs of sectioned homozygous tissue labeled with secondary 18 nm gold. Size bars measure (a-c) 2 µm; (b-d) 500nm.
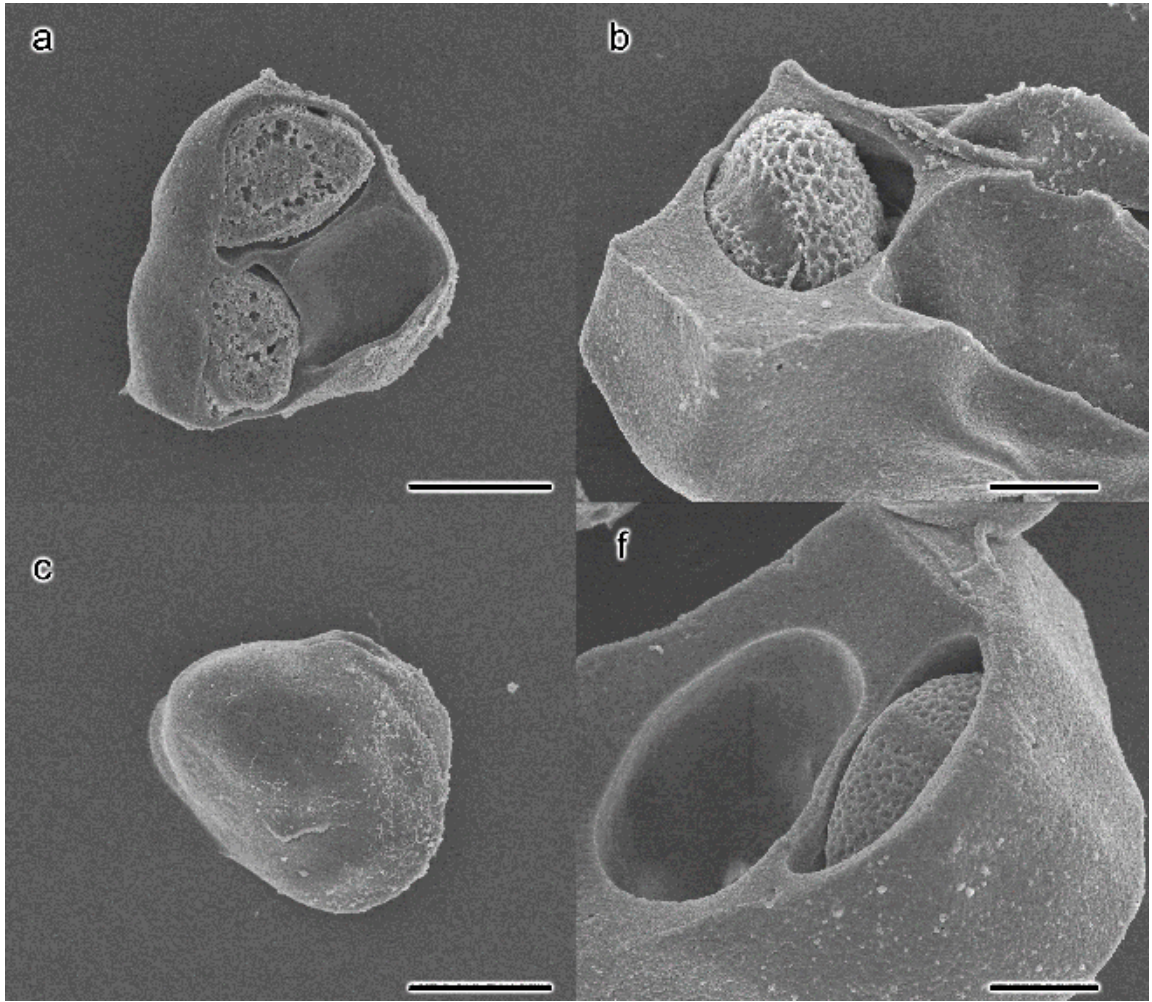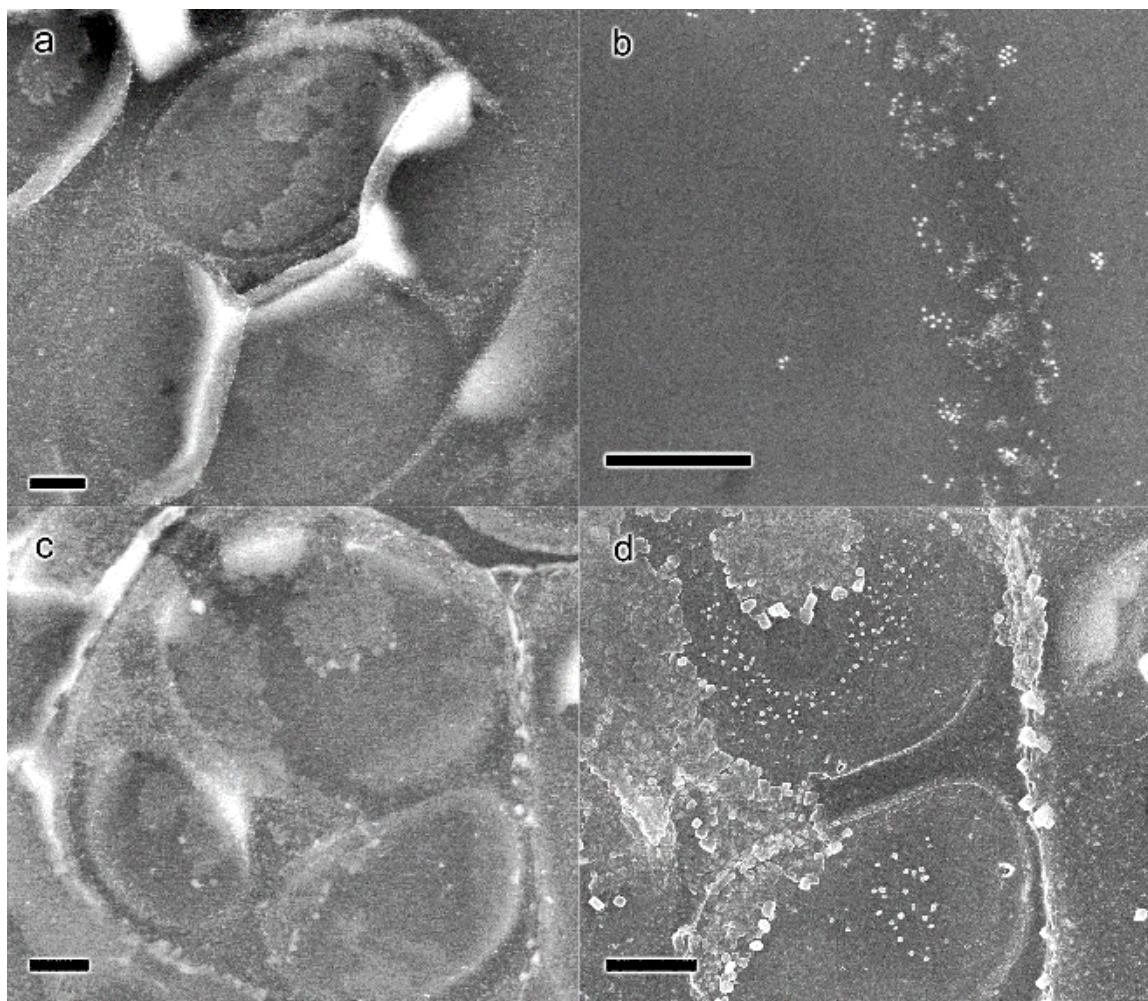
Figure 21: Analysis of enzymatic digestion of DGD Sections. (a-b) DGD sectioned tissue of *B. rapa* incubated in potassium phosphate buffer. (c-d) DGD Sectioned tissue of *B. rapa* incubated with cytohelicase in sucrose and polyvinylpyrrolidone mixture. Size bars measure 2 μm.

Chapter Six: Conclusions and Future Aspirations

To better understand the mechanisms underlying pollen wall development, a novel protocol was evaluated and later utilized to study the initiation and development of the proexine. This protocol utilized physical force in conjunction with enzymatic digestion to expose the surface of developing tetrad microspores for observation by SEM. The protocol proved effective in both microspore isolation as well as in preservation of features present at the microspore surface. This protocol was later applied to *Arabidopsis thaliana* and several known *Arabidopsis* pollen wall mutants. This technique provided unique insights into the deposition and properties of sporopollenin. We were able to observe the considerable similarity between the exine patterning established at the late tetrad stage with that of a mature grain. This similarity diverges only in the density and compression of the lacunae and tectum. When applied to the pollen wall mutants, this protocol revealed features documented in earlier studies as well as features not previously described. One such event was the observation of a polygonal patterning to the sporopollenin aggregates of the *cals5-2* and *dex1* microspores. This observation suggests the patterning may result in part from the behavior and self assembly of the sporopollenin material itself, a notion further expounded upon by Hemsley *et al*. (2005).

Additionally, the utilization of the acetolysis method furthered our understanding of early pollen development. Through the dehydration and rehydration of acetolyzed mature grains, we found evidence suggesting that the harmomegathy phenomenon requires the underlying protoplast and is not a function of the pollen wall itself. With this protocol, we were able to detect sporopollenin at the aperture regions at the tetrad stage. The acetolysis method also made apparent the presence of a developing nexine at the

tetrad stage, an observation at odds with the current literature that commonly asserts the formation of the nexine does not occur until after the release of the microspore from the callose wall. Whether this is a feature of *Brassica rapa* or all brassica species remains unclear. Additional analysis on *Arabidopsis* will need to be conducted to confirm this observation.

The analyses by SEM of the pollen wall mutants appeared to be consistent with the observations noted in previous studies. Abnormalities in development became evident in the mutant tissue at varying points of development at the tetrad stage. Microspores at the middle tetrad stage of *dex1* lacked membrane undulations. The sporopollenin deposited at this stage appeared random. Microspores of the *dex1* mutant ultimately collapsed following the dissolution of the callose wall. Microspores of *cals5-2* and *tex2-2* progressed further in development, through the middle tetrad stage, before the emergence of aberrant features. By the late tetrad stage, abnormal deposition of sporopollenin was observed in all of the mutant lines. Differences in aggregate size and distribution on the *tex2-2* microspores in comparison to the other mutants were observed. Interestingly, the presence of apertures at various stages in development was observed in all of the pollen wall mutants.

The methods developed here allow observation of the entire surface of developing microspores with the high resolution and three-dimensional qualities by scanning electron microscopy. These protocols have provided new information in the characterization of pollen wall development in both normal and mutant plants. In addition, it revealed unique features and characteristics of sporopollenin deposition and exine development not readily observed in sectioned tissue nor explicitly described in conventional literature.

Finally, it was the intent of this study to further investigate the role of the membrane protein called DEX1. Previous studies postulated that this protein play an important role in pollen development by acting as an anchoring mechanism. The localization of the protein, either at the troughs or crests of the undulating membrane, will aid in elucidating the plausible function as well as distribution of the protein throughout development. Due to the aberrant labeling with the primary antibody, this study attempted to remove the extraneous cell walls by various means. The methods evaluated were either incapable of removing the cell wall or caused severe deformation to the sample, rendering protein localization moot. It is recommended that future analyses involving the localization of DEX1 progress by employing monoclonal antibodies or through the purification of the primary antibody to alleviate the problem of non-specific labeling.

Literature:

Albert B., Raquin C., Prigent M., Nadot S., Brisset F., Yang M., and Ressayre A. (2011). Successive microsporogenesis affects pollen aperture pattern in the *tam* mutant of *Arabidopsis thaliana*. Ann. Bot. **107**: 1421– 1426.

Albini S.M., Jones G.H., and B.M.N. Wallace. (1984). A method for preparing two-dimensional surface-spreads of synaptonemal complexes from plant meiocytes for light and electron microscopy. Exp. Cell Res. **152** : 280-285.

The Arabidopsis Genome Initiative. (2000). Analysis of the genome sequence of the flowering plant *Arabidopsis thaliana*. Nature **408** : 796-815.

Arizumii, T., and Toriyama K. (2007). Pollen exine pattern formation is dependent on three major developmental processes. Intl. J. Plant Dev. Biol. **1** :106-115.

Arizumii, T., and Toriyama K. (2011). Genetic regulation of sporopollenin synthesis and pollen exine development. Annu. Rev. Plant Biol. **62** : 437–60.

Blackmore S., Wortley A.H., Skvarla J., and Rowley J.R. (2007). Pollen wall development in flowering plants. New Phytol. **174** : 483-498.

Bozzola, J.J., and Russell L.D. (1999). Electron Microscopy, 2nd. (Boston: Jones and Bartlett Publishers). pp. 262-282**.**

Capco D.G., Krochmalnic G., and Penman S. (1984). A new method of preparing embeddment-free sections for transmission electron microscopy: Applications to the cytoskeletal framework and other three dimensional networks. J. Cell Biol. **98** : 1878-1885.

Chen X.Y., and Kim J.Y. (2009). Callose synthesis in higher plants. Plant Signal. Behav. **4** : 489-492.

Clapham D.H., and Ostergren G. (1984) Immunocytochemistry of tubulin at meiosis in
Tradescantia by a protein-A gold method. Hereditas **101** : 137-142.

Cosgrove D.J. (2005). Growth of the plant cell wall. Nature. **6** : 850-861.

Dickinson H.G. (1976). Common factors in exine deposition. *In* Ferguson I.K., Muller J.
(ed.) The Evolutionary Significance of the Exine. (London: Linnean Society of
London). pp. 67-89.

Dobritsa A.A., and Coerper D. (2012). The novel plant protein INAPERTURATE
POLLEN1 marks distinct cellular domains and controls formation of apertures in
the *Arabidopsis* pollen exine. Plant Cell **24** : 4452-4464.

**Dobritsa A.A., Geanconteri A., Shrestha J., Carlson A., Kooyers N., Coerper D.,
Urbanczyk-Wochniak E., Bench B.J., Sumner L.W., Swanson R., and Preuss
D.** (2011). A large-scale genetic screen in *Arabidopsis* to identify genes involved
in pollen exine production. Plant Physiol. **157** : 947-970.

Dong X., Hong Z., Sivaramakrishnan M., Mahfouz M., and Verma D. (2005).
Callose synthase (CalS5) is required for exine formation during
microgametogenesis and for pollen viability in *Arabidopsis*. Plant J. **42** : 315-328.

Edlund A.F., Swanson R., and Preuss D. (2004). Pollen and stigma structure and
function: The role of diversity in pollination. Plant Cell **16** : S84-97.

Enns L.C., Kanaoka M.M., Torii K.U., Comai L., Okada K., and Clelend R.E.
(2005). Two callose synthases, GSL1 and GSL5, play an essential and redundant
role in plant and pollen development and in fertility. Plant Mol. Biol. **58** : 333-
349.

Feldmann K.A., and Marks M. D. (1987). *Agrobacterium*-mediated transformation of germinating seeds of *Arabidopsis thaliana*: a non tissue culture approach. Mol. Gen. Genet. **208** : 1-9.

Gabarayeva N., Grigorjeva V., Rowley J.R., and Hemsley A.R. (2009). Sporoderm development in *Trevesia burckii* (Araliaceae). I. Tetrad period: further evidence for the participation of self-assembly processes. Rev. Paleobot. Palynol. **156** : 211-232.

Hand D.T. (2007). Analysis of reduced fertility mutations in *Arabidopsis thaliana* lines that display defective pollen development. Thesis (M.S. in Biological Sciences)-University of Wisconsin-Milwaukee, 2007.

Hemsley A.R., and Gabarayeva N.I. (2005). Exine development: the importance of looking through a colloid chemistry ''window''. Plant Syst. Evol. **263** : 25–49.

Heslop-Harrison J. (1971). Pollen: Development and Physiology. (London: Butterworths & Co.). pp. 75-98.

Heslop-Harrison J. (1976). The adaptive significance of the exine. *In* Ferguson I.K., Muller J. (ed.) The evolutionary significance of the exine. (London: Linnean Society of London). pp. 27-28.

Hesse M., and Waha M. (1987). A new look at the acetolysis method. Plant Syst. Evol. **163** : 141-152.

Hill J., and Lord, E. (1989). Floral development in *Arabidopsis thaliana*: A comparison of the wild type and the homeotic pistillata mutant. Can. J. Bot. **67** : 2922-2936.

Jiang J., Zhang, Z., and Cao J. (2013). Pollen wall development: the associated enzymes and metabolic pathways. Plant Biol. **15** : 249–263.

Jones T.P., and Rowe N.P. (1999). Fossil Plants and Spores: Modern Techniques. (London: The Geological Society Publishing House). pp.28-29.

Kostic E.L. (2002). Localization and calcium binding studies of DEX1 from *Arabidopsis thaliana.* Thesis (M.S.)--Miami University, Dept. of Chemistry and Biochemistry, 2002.

Lersten N.R. (2004). Flowering Plant Embryology. (Ames: Blackwell Publishing). pp. 10-20.

Liu L., and Fan X.D. (2013). Tapetum: regulation and role in sporopollenin biosynthesis in Arabidopsis. Plant Mol. Biol. **83** : 165–175.

Ma, H. (2005). Molecular genetic analyses of microsporogenesis and microgametogenesis in flowering plants. Annu. Rev. Plant Biol. **56** : 393-434.

Matveyeva N.P., Polevova S.V., Smirnova A.V., Yermakov I.P. (2012) Sporopollenin accumulation in *Nicotiana tabacum* L. microspore wall during its development. Cell Tissue Biol. **6** : 293-301.

Nickerson J.A., Krockmalnic G., He D. and Penman S. (1990). Immunolocalization in three dimensions: Immunogold staining of cytoskeletal and nuclear matrix proteins in resinless electron microscopy sections. Cell Biol. **87** : 2259-2263.

Nishikawa S., Zinkl G.M., Swanson R.J., Maruyama D., and Preuss D. (2005). Callose (beta-1,3 glucan) is essential for Arabidopsis pollen wall patterning, but not tube growth. BMC Plant Biology 5 : 22.

Otegui M.S, and L.A. Staehelin. (2004). Electron tomographic analysis of post-meiotic cytokinesis during pollen development in *Arabidopsis thaliana*. Planta **218** : 501-515.

Owen H.A., and Makaroff C.A. (1995). Ultrastructure of microsporogenesis and microgametogenesis in *Arabidopsis thaliana* L. Heynh. ecotype Wassilewskija (Brassicaceae). Protoplasma **185** : 7-21.

Paxinos R., and Mitchell J.G. (2000). A rapid Utermöhl method for estimating algal numbers. J. Plankton Res. **22** : 2255-2262.

Paxson-Sowders D.M., Dodrill C.H., Owen H.A., and Makaroff C.A. (2001). DEX1, a novel plant protein, is required for exine pattern formation during pollen development in *Arabidopsis*. Plant Physiol. **127** : 1739–1749.

Paxson-Sowders D.M., Owen H.A., Makaroff C.A. (1997). A comparative ultrastructural analysis of exine pattern development in wild-type *Arabidopsis* and a mutant defective in pattern formation. Protoplasma **198** : 53–65.

Peirson B.N., Bowling S.E., and Makaroff C.A. (1997). A defect in synapsis causes male sterility in a T-DNA-tagged *Arabidopsis thaliana* mutant. Plant J. **11** : 659-669.

Robles, P., and Pelaz, S. (2005). Flower and fruit development in *Arabidopsis thaliana*. Int. J. Dev. Biol. **49** : 633-643.

Ross K.J., Fransz P., and Jones G.H. (1996). A light microscopic atlas of meiosis in *Arabidopsis thaliana*. Chromosome Res. 4, 507-516.

Rowley J., and Skvarla J. (2000). The elasticity of the exine. Grana **39** : 1, 1-7.

Sanders P.M., Bui A.Q., Weterings K., McIntire K.N., Hsu Y., Lee P.Y., Truong M.T., Beals T.P., and Goldberg R.B. (1999). Anther developmental defects in *Arabidopsis thaliana* male-sterile mutants. Sex. Plant Reprod. **11** : 297-322.

Smallwood M., Martin H., and Knox J.P. (1995) An epitope of rice threonine- and hydroxyproline-rich glycoprotein is common to cell wall and hydrophobic plasma-membrane glycoproteins. *Planta* **196** : 510-522.

Swatzell L.J., Edelmann R.E., Makaroff C.A. and Kiss J.Z. (1999). Integrin-like proteins are localized to plasma membrane fractions, not plastids, in *Arabidopsis*. Plant Cell Physiol. **40** : 173-183.

Takahashi M. (1980). On the development of the reticulate structure of *Hemerocallis* pollen (Liliaceae). Grana **19** : 3-5.

Takahashi M., and Skvarla J.J. (1991). Exine pattern formation by plasma membrane in *Bougainvillea spectabilis* Willd. (Nyctaginaceae). Am. J. Bot. **78** : 1063-1069.

Taleporos P. (1974). Diethylene glycol distearate as an embedding medium for high resolution light microscopy. J. Hystochem. Cytochem. **22** : 29-34.

Vaughn K. (2013). Immunocytochemistry of plant cells. (Salem: Springer Science+Business Media). pp. 19-27.

Volkova O.A., Severova E.E., and Polevova S.V. (2013). Structural basis of harmomegathy: evidence from *Boraginaceae* pollen. Plant Syst. Evol. **229** : 1769-1779.

Wallace S., Fleming A., Wellman C.H., Berling D. (2011). Evolutionary development of the plant spore and pollen wall. AoB Plants 2011, plr027.

Wick S.M. (1993). Immunolabeling of antigens in plant cells. *In* DJ Asai (ed.) Methods in cell biology. (San Diego: Academic Press). pp. 171-200.

Zhou Q., Zhu J., Cui Y., and Yang Z. Ultrastructure analysis reveals sporopollenin deposition and nexine formation at early stage of pollen wall development in *Arabidopsis*. Science Bulletin. **2** : 273-276.